J. Biochem. 2009;146(6)881–886
doi:10.1093/jb/mvp135

FGF-1-Induced Reactions for Biogenesis of apoE-HDL are Mediated by Src in Rat Astrocytes

Tomo Nishida, Jin-ichi Ito, Yuko Nagayasu and Shinji Yokoyama*

Biochemistry, Nagoya City University Graduate School of Medical Sciences, Kawasumi 1, Mizuho-cho, Mizuho-ku, Nagoya 467-8601, Japan

Received July 8, 2009; accepted August 18, 2009; published online August 27, 2009

Fibroblast growth factor-1 (FGF-1) is released from astrocytes in stress and stimulates MEK/ERK and PI3K/Akt pathways in autocrine fashion to increase synthesis of cholesterol and 25-OH-cholesterol, and to induce transport and secretion of apoE, respectively. FGF-1-induced phosphorylation of Src, and phosphorylation of MEK, ERK and Ark was inhibited by Src inhibitors in rat astrocytes. Src inhibitors also suppressed FGF-1-induced increase of biosynthesis and release of cholesterol and increase of apolipoprotein E (apoE) secretion. The results were reproduced in rat astrocytoma cells transfected by rat apoE and in 3T3-L1 cells. Down-regulation of Src expression reduced FGF-1-induced phosphorylation of the signalling protein and subsequent reactions. Increase by FGF-1 of messages of apoE and HMG-CoA reductase was not influenced by Src inhibitors or by its down-regulation. We conclude that FGF-1 activates Src for activation of MEK/ERK and PI3K/Akt pathways, while Src may not be involved in enhancement of transcription of the cholesterol-related genes.

Key words: Astrocytes, apolipoprotein E, high density lipoprotein, fibroblast growth factor-1, Src.

Abbreviations: apo, apolipoprotein; CNS, Central nervous system; FGF-1, fibroblast growth factor-1; FGFR1, FGF receptor 1; HDL, high density lipoprotein; PKB, protein kinase B; siRNA, small interfering RNA; TCA, trichloroacetic acid; TLC, thin layer chromatography.

Central nervous system (CNS) is segregated from systemic blood circulation by blood brain barrier, which plasma lipoproteins do not cross, so that CNS uses its own intercellular lipid transport system by high-density lipoprotein (HDL) (*1*). Astrocytes are the main HDL supplier in CNS with apolipoprotein E (apoE) synthesized by astrocytes themselves (*2*, *3*) and extracellular apoA-I from unknown sources (*4*, *5*).

ApoE production increases in the brain in the cases of injury and damage, acutely and perhaps chronically as well, such as cerebral infarction, nerve and brain injury and their degeneration (*6–15*). We found that healing of the experimental cryo-injury of the brain was substantially retarded in the apoE-deficient mice (*16*). Production of fibroblast growth factor-1 (FGF-1) was observed in astrocytes in the peri-injury regions 2 days after the injury, both in the apoE-deficient and wild-type mice brain. ApoE production increased a few days later in the same regions of the wild-type mouse brain (*16*). FGF-1 is produced and released by astrocytes in culture and stimulates the astrocytes for apoE-HDL production (*17*, *18*). We further demonstrated that FGF-1 induces phosphorylation of the PI3K/Akt pathway for apoE transport and secretion and the phosphorylation of the MEK/ERK pathway for lipid biosynthesis via the FGF receptor(s) (*19*). FGF-1 stimulates MEK/ERK pathways also for production of 25-OH-cholesterol to activate LXRα for the apoE gene expression (*20*). On the other hand, c-Src, reportedly regulates physiological activities of FGF-1 such as proliferation of murine embryonic fibroblasts (*21*).

In the present work, we investigated the involvement of Src in an initial step(s) of the FGF-1-induced reactions of cholesterol biosynthesis, cholesterol release and apoE secretion and found that activation of Src protein is critically involved in activation of MEK/ERK and PI3K/Akt pathways in their upstream.

MATERIALS AND METHODS

Reagents—SU5402, an inhibitor of FGF receptor-1 (FGFR1) was purchased from Calbiochem. Src inhibitors (PP1 and SU6656) were obtained from BIOMOL and Calbiochem, respectively.

Preparation of Rat Astrocytes—Astrocytes were prepared from the 17-day-old fetal brain of Wistar rat according to the method described previously (*22*). Rat apoE/pcDNA3.his was transfected to transformed rat astrocyte GA-1 cells (*23*) that otherwise do not synthesize apoE (GA-1/25) (*19*). Mouse fibroblast 3T3-L1 cells were obtained from Riken Cell Bank. The cells were washed and incubated in 0.1% BSA/F-10 for 16 h before each experimental use.

Synthesis and Release of Cellular Cholesterol—To measure *de novo* synthesis of cholesterol, astrocytes were incubated with [^{14}C]-acetate (4 μCi/ml) for 2 h, lipid was

*To whom correspondence should be addressed.
Tel: +81-52-853-8139, Fax: +81-52-841-3480,
E-mail: syokoyam@med.nagoya-cu.ac.jp

extracted from the cells with hexane/isopropanol (3 : 2, v/v) and radioactivity was counted in cholesterol after separation by thin layer chromatography (TLC) (*22*). To determine cholesterol released into the medium, astrocytes were labelled by incubating with [^{14}C]-acetate (4 μCi/ml) for 24 h, washed three times and incubated in a fresh 0.02% BSA/F-10 for 6 h (*22*). Lipid was extracted from the medium with chloroform/methanol (2 : 1, v/v) and analysed by TLC to count radioactivity in cholesterol.

Analysis of Protein by Western blotting—The method was described previously (*19*). Protein in the conditioned medium, cytosol and membrane fraction was precipitated with 10% trichloroacetic acid (TCA) for the analysis of its 70 μg in 10% SDS–PAGE and immunoblotting with rabbit antibodies against rat apoE (a generous gift by Dr J. Vance, The University of Alberta), phosphorylated Akt (Thr-308) (Cell Signaling Technology), p44/42 MAP kinase (Cell Signaling Technology), phosphorylated MEK 1/2 (Ser217/221) (Cell Signaling Technology), MEK 1/2 (Cell Signaling Technology), mouse antibodies against protein kinase B (PKB)α/Akt (BD Transduction Laboratories), phosphorylated p44/p42 MAP kinase (Thr202/Tyr204) (Cell Signaling Technology), phosphorylated Src (Tyr416) (Upstate), Src (Upstate) and a goat antibody against FGF-1 (Santa Cluz Biotechnology).

Reverse Transcriptase Polymerase Chain Reaction—Total cellular RNA was isolated using ISOGEN (Nippon Gene) and subjected to reverse transcription to cDNA by Thermo Script (Invitrogen) with oligo-dT primers and amplification of cDNA by using the primers for apoE, HMG-CoA reductase, β-actin in a Gene Amp (Applied Biosystems). After an electrophoresis of the products in agarose gels, the bands were stained with EtBr solution (Nippon Gene Co. Ltd, Tokyo) and visualized by an ultraviolet transilluminator (UVP NML-20 E) at 302 nm. The primer pairs used were: 5′-ctgttggtcccattg ctgac-3′ (sense) and 5′-tgtgtgacttgggagctctg-3′ (antisense) for apoE; 5′-tgctgctttggctgtatgtc-3′ (sense) and 5′tgagcgtg aacaagaaccag-3′ (antisense) for HMG-CoA reductase. β-Actin primers were used as an internal control (*19*).

RNA Interference—Specific small interfering RNA (siRNA) for rat Src and universal control were obtained from Invitrogen and transfected into rat astrocytes using Lipofectamine RNAiMAX (Invitrogen) according to the manufacturer's protocol. After transfection, cells were harvested and subsequently mRNA expression and proteins were analyzed.

RESULTS

Signalling pathways by FGF-1 stimulation were investigated in rat astrocytes. Figure 1A demonstrates phosphorylation of the signal proteins MEK, ERK, Akt and Src. As reported previously (*19*), MEK, ERK and Akt proteins were phosphorylated by FGF-1 stimulation. In addition to those, Src protein was also phosphorylated by FGF-1 stimulation. These protein phosphorylation were all inhibited by an FGFR1 inhibitor SU5402 (Fig. 1A), showing that the reactions including Src phosphorylation were mediated by FGF-1 and its receptors. Figure 1B shows that phosphorylation of the signal proteins was inhibited by Src inhibitors, PP1 and SU6656.

FGF-1 induces signals of the PI3K/Akt pathway for apoE transport/secretion and the MEK/ERK pathway for lipid biosynthesis via the FGF receptor(s) (*19*, *24*). We therefore investigated involvement of Src in the FGF-1-induced cholesterol biosynthesis, cholesterol release and apoE secretion. Figure 1C demonstrates that Src inhibitors, SU6656 and PP1, inhibited cholesterol biosynthesis and its release induced by FGF-1. It is also shown that increase of apoE secretion by FGF-1 was inhibited by Src inhibitors. Thus, the findings were consistent with the effects of Src inhibitors on the MEK/ERK and PI3/Akt pathways, showing the involvement of Src phosphorylation in the upstream of signal activations in the FGF-1-induced reactions in astrocytes.

Involvement of Src in the signalling pathways was confirmed in the cell line cells. We used rat astrocyte cell line GA-1/25 cells, transformed rat astrocytes to which rat apoE/pcDNA3.his was transfected (*19*), and also mouse fibroblasts 3T3-L1. FGF-1-induced phosphorylation of MEK, ERK and Akt in GA-1/25 and 3T3-L1 cells (Fig. 2A and B). The phosphorylations in GA-1/25 cells were suppressed by Src inhibitors SU6656 and PP1, and those were inhibited by an FGF-1 receptor inhibitor SU5402 and by SU6656 and PP1 in 3T3-L1 cells (Fig. 2A and B). Secretion of apoE from GA-1/25 cells was increased by FGF-1 and the increase was reversed by SU6656 and PP1, indicating that Src is involved in the FGF-1-mediated reactions independent of transcriptional regulation of apoE (Fig. 2C). Cholesterol biosynthesis in GA-1/25 cells and its increase by FGF-1 were severely inhibited by SU6656 and PP1, indicating the presence of basic activation of Src in this cell line cells (Fig. 2D).

FGF-1 induces the increase of mRNA of the lipid-related genes such as apoE and HMG-CoA reductase, in time-dependent manners (Fig. 3A). Interestingly, neither Src inhibitors, SU6656 nor PP1, influenced these increases (Fig. 3B). Therefore, induction of these genes by FGF-1 does not involve Src activation, unlike induction of signalling pathways of MEK/ERK and PI3K/Akt for up-regulation of synthesis of cholesterol/25-OH-cholesterol (*20*) and enhancement of transport/secretion of apoE (*19*, *20*).

Involvement of Src in activation of the signalling pathways was further investigated by down-regulation of the Src gene using a specific siRNA. Figure 4A showed that down-regulation of the Src gene was saturated at 200 nM of siRNA so that this concentration was used thereafter. Src protein expression was almost completely suppressed in this condition (Fig. 4B). Phosphorylation of MEK, ERK and Akt were all reduced by the siRNA treatment of the cells (Fig. 4C). Under the same condition, the expression of the genes of apoE and HMG-CoA reductase was not significantly influenced at all (Fig. 4D).

DISCUSSION

ApoE is the major endogenous apolipoprotein in CNS, synthesized and secreted by astrocytes and microglias to form apoE-HDL (*1*). Production of apoE and apoE-HDL increases in response to acute and chronic

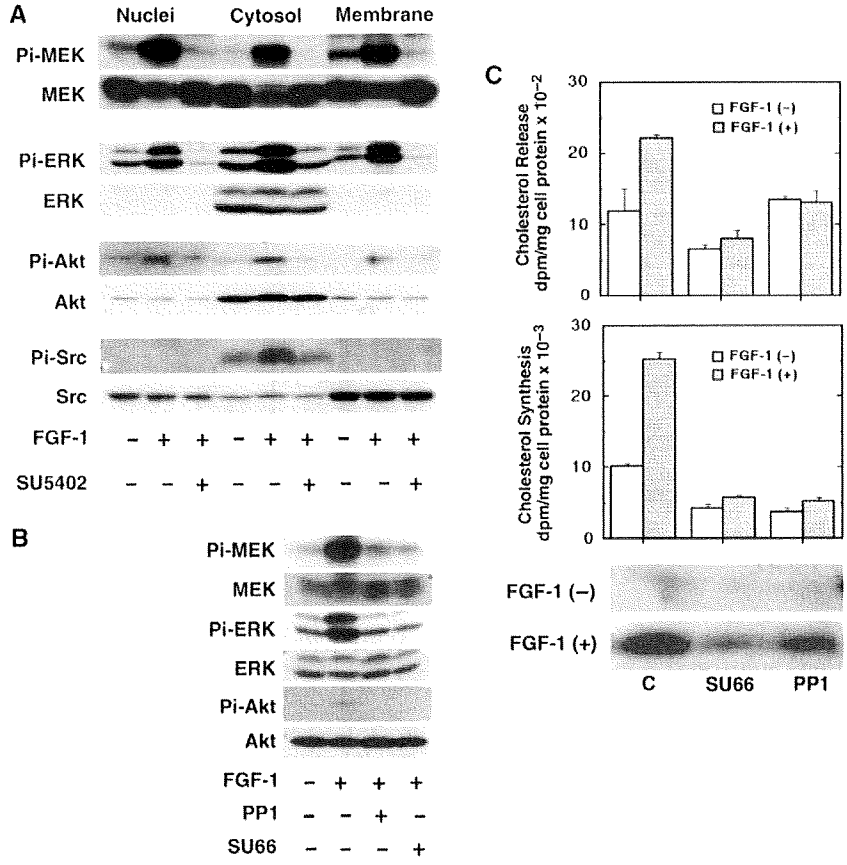

Fig. 1. **Involvement of the FGF-1 receptor and Src in the FGF-1-induced reactions in astrocytes.** (A) Rat astrocytes were pre-treated with the FGF-1 receptor inhibitor (SU5402, 10 μM) for 1 h, and stimulated with FGF-1 (50 ng/ml) for 5min. Cytosol and membrane fractions were prepared, and protein of each fraction was analysed by western blotting for MEK, ERK, Akt and Src proteins and their phosphorylated form (Pi). (B) The cells were pre-treated with Src inhibitors (PP1 or SU6656, 10 μM) for 1 h and stimulated by FGF-1 (50 ng/ml) for 5min. Cell protein was analysed by western blotting for the signal proteins and their phosphorylated form (Pi). (C) Cellular cholesterol release was measured in the presence of FGF-1 (50 ng/ml), SU6656 (10 μM) or PP1 (10 μM) (Top). Cholesterol biosynthesis was determined upon incubation with SU6656 (10 μM) or PP1 (10 μM) for 1 h and then with FGF-1 (0 or 50 ng/ml) for 5 h (Middle). ApoE secretion was measured under stimulation with FGF-1 (0 or 100 ng/ml) for 24 h in the presence of SU6656 (5 μM) or PP1 (5 μM). The conditioned medium was analysed by western blotting for apoE.

damage of CNS, and seems to play a role in regeneration of nerve cells and healing of the injury (*6–15*). Therefore, it is important to understand the background of molecular mechanism for this reaction and the recovery process of the brain damage. We discovered that apoE-HDL production is stimulated by FGF-1 in astrocytes by an autocrine mechanism and helps healing of the brain cryo-injury (*16–19*). FGF-1 up-regulates apoE-HDL biogenesis by using at least three independent signalling pathways, a PI3K/Akt pathway for transport/secretion of apoE, an MEK/ERK pathway for cholesterol and lipid biosynthesis, and an independent pathway for apoE transcription (*19*). All of these pathways are probably initiated by the interaction of FGF-1 with its receptors (*19*, *20*).

We here characterized the involvement of Src in these FGF-1-induced signalling pathways. The results are summarized as follows (Fig. 5): (i) FGF-1-induced phosphorylation of MEK, ERK, Akt and Src proteins and these phosphorylations were inhibited by an inhibitor of the FGF-1 receptor. (ii) FGF-1-induced phosphorylation of MEK, ERK and were all inhibited by Src inhibitors and by siRNA of Src, and FGF-1-induced cholesterol synthesis, cholesterol release and apoE secretion were inhibited by Src inhibitors. (iii) Induction by FGF-1 of the genes related to lipid metabolism was not inhibited either by Src inhibitors or by Src siRNA. We concluded that FGF-1 induces MEK, ERK and Akt phosphorylation and cholesterol synthesis, cholesterol release and apoE secretion being mediated by the Src kinase. In this FGF-1-induced signalling pathway, Src seems located downstream of the FGFR1 and upstream of the MEK/ERK and PI3K pathways. Furthermore, these data showed that induction of the genes related to lipid metabolism such as apoE and HMG-CoA reductase is independent of the Src pathway.

We recently demonstrated that induction of apoE gene by FGF-1 is under the dual control, by the MEK/ERK

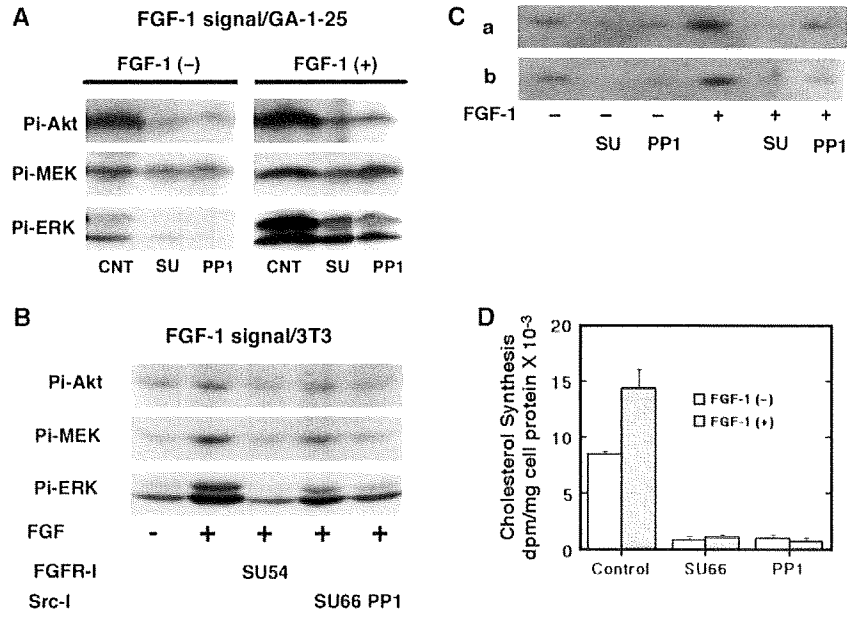

Fig. 2. **Involvement of the FGF-1 receptor and Src in the FGF-1-induced reactions in astrocytes in rat astrocytoma cells and mouse fibroblast.** (A) Inhibition of the FGF-1-induced reactions by Src inhibitors in GA-1/25 cells. The cells were stimulated with FGF-1 (50 ng/ml) for 5 min after pre-treatment with the Src inhibitors (PP1 or SU6656, 10 μM) for 1 h. The cell protein was analysed by western blotting for phosphorylated forms of MEK, ERK and Akt (Pi). (B) Inhibition of the FGF-1-induced reactions by the inhibitors of the FGF-1 receptor or Src in 3T3-L1 cells. The cells were stimulated with FGF-1 (50 ng/ml) for 5 min after pre-treatment with SU5402, PP1 or SU6656, 10 μM, for 1 h. Cell protein was analysed by western blotting for phosphorylated forms of MEK, ERK and Akt (Pi). (C) Inhibition of the FGF-1-induced secretion of apoE by Src inhibitors in GA-1/25 cells. After 16 h blank incubation, the cells were stimulated with FGF-1 (0 or 50 ng/ml) for 24 h in the presence SU6656 (5 μM) or PP1 (5 μM), and further incubated for 16 h (a). The cells were incubated with FGF-1 (0 or 50 ng/ml) for 24 h, then with SU6656 (5 μM) or PP1 (5 μM) for 16 h, and further incubated for 16 h (b). The conditioned medium was analysed by western blotting for apoE. (D) Inhibition of the FGF-1-induced cholesterol synthesis by Src inhibitors. GA-1/25 cells were incubated with SU6656 (10 μM) or PP1 (10 μM) for 1 h and then with FGF-1 (0 or 50 ng/ml) for 5 h. Cholesterol synthesis was determined as described in the text.

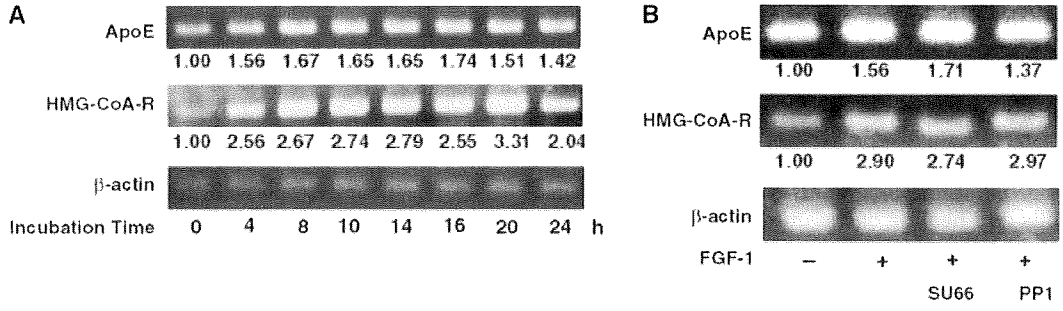

Fig. 3. **Expression of mRNA of the lipid metabolism-related genes induced by FGF-1 in rat astrocytes.** (A) mRNA expression of the lipid-related genes in a time course. Rat astrocytes were stimulated with 50 ng/ml of FGF-1 for the time indicated. Total RNA was extracted and subjected to reverse transcription and cDNA amplification for apoE, HMG-CoA reductase and β-actin. (B) Effect of Src inhibitors on mRNA expression of the lipid-related genes. Rat astrocytes were stimulated with 50 ng/ml of FGF-1 for 8 h after pre-treatment with Src inhibitors (PP1, SU6656) for 1 h. Total RNA was extracted and subjected to reverse transcription and cDNA amplification for apoE, HMG-CoA reductase and β-actin. Each band was digitally scanned by using an EPSON GT-X700 and Adobe Photoshop software. Numbers below each band indicates relative increase of its intensity from the controls after standardized for β-actin.

pathway to induce synthesis of cholesterol and 25-OH-cholesterol to activate LXRα and by induction of the LXRα gene through an unknown signalling pathway (*20*). The present results provided somewhat confusing information for understanding the differential signalling network for induction of biogenesis of apoE-HDL by FGF-1 in astrocytes. (i) Although the increase of cholesterol biogenesis is mediated by the MEK/ERK pathway (*19*) and it is suppressed by inhibiting Src, induction of HMG-CoA reductase by FGF-1 seems independent of this

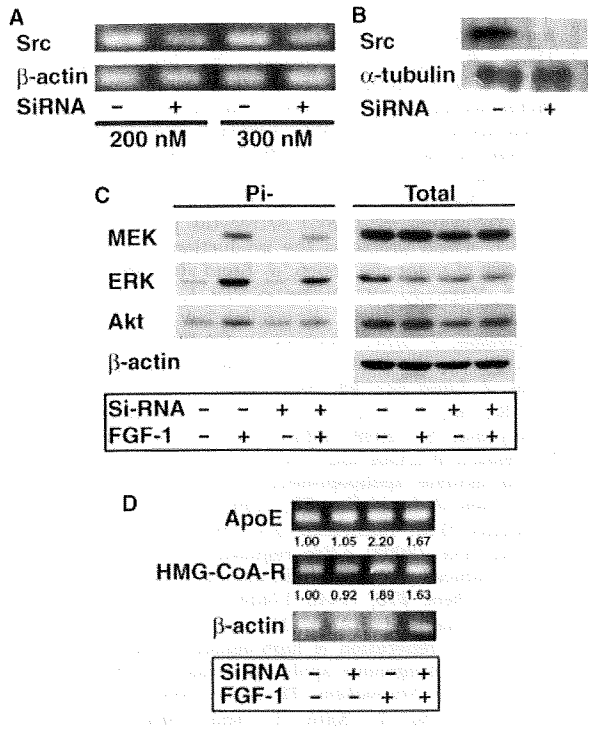

Fig. 4. **Effect of the treatment with Src siRNA.** (A) Effect of siRNA on expression of Src. Rat astrocytes were incubated with fresh Opti-mem for 10 h and then incubated with Src RNAi at 200 nM and 300 nM for 24 h. Total RNA was extracted and subjected to reverse transcription and cDNA amplification by using primer pairs for Src as described in the text. (B) Effect of Src siRNA on expression of Src protein. Rat astrocytes were incubated with fresh Opti-mem for 10 h and then incubated with 200 nM Src RNAi for 24 h. The cytosol protein was analysed by western blotting for α-tublin protein. (C) Rat astrocytes were pre-treated with 200 nM Src siRNA as above. After 5 min stimulation by FGF-1, cell protein was analysed by western blotting for MEK, ERK, Akt and their phosphorylated form (Pi). (D) Rat astrocytes were pre-treated with 200 nM Src RNAi as above. The cells were incubated with FGF-1 for 8 h and total RNA was subjected to reverse transcription and cDNA amplification by using primer pairs for apoE, HMG-CoA reductase and β-actin. Each band was digitally scanned by using an EPSON GT-X700 and Adobe Photoshop software. Numbers below each band indicates relative increase of its intensity from the controls after standardized for β-actin.

pathway indicating that cholesterol biosynthesis is stimulated by FGF-1 at an other step(s) than HMG-CoA reductase as well. (ii) Although expression of the apoE gene is induced by FGF-1 through production of cholesterol and 25-OH-cholesterol via the MEK/ERK pathway (*20*), LXRα induction directly increases the apoE gene transcription independently of this pathway (*19*). This view is consistent with the previous suggestion that enhancement of cholesterol biosynthesis by FGF-1 is due to the demand by stimulation of cell growth (*25*). Induction of the apoE gene transcription by FGF-1 may not all necessarily be associated with cholesterol biosynthesis and shown to be partially independent of either PI3K/Akt or MEK/ERK pathways as mentioned earlier (*19*).

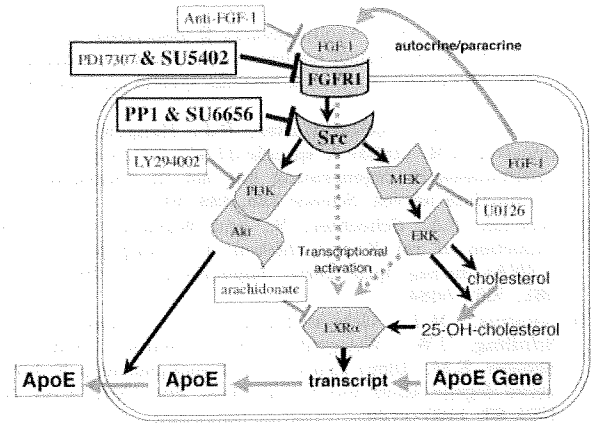

Fig. 5. **Schematic diagram for signalling pathways for FGF-1 to stimulate production of apoE-HDL in rat astrocytes.** FGF-1 is released by astrocytes in the lesions of brain damage and stimulates those cells in autocrine/paracrine fashion (*16–18*). This stimulation is mediated by FGFR1, and subsequently uses the MEK/ERK pathway to increase the synthesis of cholesterol and 25-OH-cholesterol, activate LXRα and enhance transcription of the apoE gene, and the PI3K/Akt pathway to increase apoE-HDL secretion (*19*, *20*). FGF-1 also enhances production of LXRα being independent of the aforementioned pathways (*19*, *20*). Src was shown to mediate signals from FGFR1 to the MEK/ERK and P13K/Akt pathways.

FUNDING

This study was supported by International HDL Award Program, in part by grants-in-aid from The Ministries of Education, Science, Technology, Culture and Sports, and of Health, Welfare and Labour of Japan, and by the Program for Promotion of Fundamental Studies in Health Sciences of National Institute of Biomedical Innovation.

CONFLICT OF INTEREST

None declared.

REFERENCES

1. Ito, J. and Yokoyama, S. (2004) *Non-neural Cells of the Nervous System: Function and Dysfunction* (Hertz, L., ed.), pp. 519–534, Elsevier, Amsterdam
2. Pitas, R.E., Boyles, J.K., Lee, S.H., Foss, D., and Mahley, R.W. (1987) Astrocytes synthesize apolipoprotein E and metabolize apolipoprotein E-containing lipoproteins. *Biochim. Biophys. Acta* **917**, 148–161
3. Nakai, M., Kawamata, T., Taniguchi, T., Maeda, K., and Tanaka, C. (1996) Expression of apolipoprotein E mRNA in rat microglia. *Neurosci. Lett.* **211**, 41–44
4. Weiler-Guttler, H., Sommerfeldt, M., Papandrikopoulou, A., Mischek, U., Bonitz, D., Frey, A., Grupe, M., Scheerer, J., and Gassen, H.G. (1990) Synthesis of apolipoprotein A-I in pig brain microvascular endothelial cells. *J. Neurochem.* **54**, 444–450
5. Mockel, B., Zinke, H., Flach, R., Weis, B., Weiler-Guttler, H., and Gassen, H.G. (1994) Expression of apolipoprotein A-I in porcine brain endothelium in vitro. *J. Neurochem.* **62**, 788–798

6. Boyles, J.K., Pitas, R.E., Wilson, E., Mahley, R.W., and Taylor, J.M. (1985) Apolipoprotein E associated with astrocytic glia of the central nervous system and with nonmyelinating glia of the peripheral nervous system. *J. Clin. Invest.* **76**, 1501–1513
7. Muller, H.W., Gebicke-Harter, P.J., Hangen, D.H., and Shooter, E.M. (1985) A specific-37,000-dalton protein that accumulates in regenerating but not in nonregenerating mammalian nerves. *Science* **228**, 499–501
8. Dawson, P.A., Schechter, N., and Williams, D.L. (1986) Induction of rat E and chicken A-I apolipoproteins and mRNAs during optic nerve degeneration. *J. Biol. Chem.* **261**, 5681–5684
9. Ignatius, M.J., Gebicke-Harter, P.J., Skene, J.H.P., Schilling, J.W., Weisgraber, K.H., Mahley, R.W., and Shooter, E.M. (1986) Expression of apolipoprotein E during nerve degeneration and regeneration. *Proc. Natl Acad. Sci. USA* **83**, 1125–1129
10. Snipes, G.J., McGuire, C.B., Norden, J.J., and Freeman, J.A. (1986) Nerve injury stimulates the secretion of apolipoprotein E by nonneuronal cells. *Proc. Natl Acad. Sci. USA* **83**, 1130–1134
11. Mahley, R.W. (1988) Apolipoprotein E: Cholesterol transport protein with expanding role in cell biology. *Science* **240**, 622–630
12. Harel, A., Fainaru, M., Shafer, Z., Hernandez, M., Cohen, A., and Schwartz, M. (1989) Optic nerve regeneration in adult fish and apolipoprotein A-I. *J. Neurochem.* **52**, 1218–1228
13. Graham, D.I., Horsburgh, K., Nicoll, J.A., and Trasdale, G.M. (1999) Apolipoprotein E and the response of the brain to injury. *Acta Neurochir. Suppl.* **73**, 89–92
14. Haasdijk, E.D., Vlug, A., Mulder, M.T., and Jaarsma, D. (2002) Increased apolipoprotein E expression correlates with the onset of neuronal degeneration in the spinal cord of G93A-SOD1 mice. *Neurosci. Lett.* **335**, 29–33
15. Aoki, K., Uchihara, T., Sanjo, N., Nakamura, A., Ikeda, K., Tsuchiya, K., and Wakayama, Y. (2003) Increased expression of neuronal apolipoprotein E in human brain with cerebral infarction. *Stroke* **34**, 875–880
16. Tada, T., Ito, J., Asai, M., and Yokoyama, S. (2004) Fibroblast growth factor 1 is produced prior to apolipoprotein E in the astrocytes after cryo-injury of mouse brain. *Neurochem. Int.* **45**, 23–30
17. Ueno, S., Ito, J., Nagayasu, Y., Furukawa, T., and Yokoyama, S. (2002) An acidic fibroblast growth factor-like factor secreted into the brain cell culture medium upregulates apoE synthesis, HDL secretion and cholesterol metabolism in rat astrocytes. *Biochim. Biophys. Acta* **1589**, 261–272
18. Ito, J., Nagayasu, Y., Lu, R., Kheirollah, A., Hayashi, M., and Yokoyama, S. (2005) Astrocytes produce and secrete FGF-1, which promotes the production of apoE-HDL in a manner of autocrine action. *J. Lipid Res.* **46**, 679–686
19. Ito, J., Nagayasu, Y., Okumura-Noji, K., Lu, R., Nishida, T., Miura, Y., Asai, K., Kheirollah, A., Nakaya, S., and Yokoyama, S. (2007) Mechanism for FGF-1 to regulate biogenesis of apolipoprotein E-high density lipoprotein in astrocytes. *J. Lipid Res.* **48**, 2020–2027
20. Lu, R., Ito, J., Iwamoto, N., Nishimaki-Mogami, T., and Yokoyama, S. (2009) Fibroblast growth factor-1 induces expression of LXRa and production of 25-hydroxycholesterol to up-regulate apolipoprotein E gene transcription in rat astrocytes. *J. Lipid Res.* **50**, 1156–1164
21. Kilkenny, D.M., Rocheleau, J.V., Price, J., Reich, M.B., and Miller, G.G. (2003) c-Src regulation of fibroblast growth factor-induced proliferation in murine embryonic fibroblasts. *J. Biol. Chem.* **278**, 17448–17454
22. Ito, J., Zhang, L., Asai, M., and Yokoyama, S. (1999) Differential generation of high-density lipoprotein by endogenous and exogenous apolipoproteins in cultured fetal rat astrocytes. *J. Neurochem.* **72**, 2362–2369
23. Zhang, L., Ito, J., Kato, T., and Yokoyama, S. (2000) Cholesterol homeostasis in rat astrocytoma cells GA-1. *J. Biochem.* **128**, 837–845
24. Hashimoto, M., Sagara, Y., Langford, D., Everall, I.P., Mallory, M., Everson, A., Digicaylioglu, M., and Masliah, E. (2002) Fibroblast growth factor 1 regulates signaling via the glycogen synthase kinase-3beta pathway. Implications for neuroprotection. *J. Biol. Chem.* **277**, 32985–32991
25. LaVallee, T.M., Prudovsky, I.A., McMahon, G.A., Hu, X., and Maciag, T. (1998) Activation of the MAP kinase pathway by FGF-1 correlates with cell proliferation induction while activation of the Src pathway correlates with migration. *J. Cell Biol.* **141**, 1647–1658

Arteriosclerosis, Thrombosis, and Vascular Biology

JOURNAL OF THE AMERICAN HEART ASSOCIATION

ApoA-I Facilitates ABCA1 Recycle/Accumulation to Cell Surface by Inhibiting Its Intracellular Degradation and Increases HDL Generation

Rui Lu, Reijiro Arakawa, Chisato Ito-Osumi, Noriyuki Iwamoto and Shinji Yokoyama

Arterioscler Thromb Vasc Biol 2008;28;1820-1824; originally published online Jul 10, 2008;
DOI: 10.1161/ATVBAHA.108.169482
Arteriosclerosis, Thrombosis, and Vascular Biology is published by the American Heart Association. 7272 Greenville Avenue, Dallas, TX 72514
 Print ISSN: 1079-5642. Online ISSN: 1524-4636

ApoA-I Facilitates ABCA1 Recycle/Accumulation to Cell Surface by Inhibiting Its Intracellular Degradation and Increases HDL Generation

Rui Lu, Reijiro Arakawa, Chisato Ito-Osumi, Noriyuki Iwamoto, Shinji Yokoyama

Objective—Calpain-mediated proteolysis is one of the major regulatory factors for activity of ATP-binding cassette transporter (ABC) A1. Helical apolipoproteins protect ABCA1 against this degradation and increase generation of HDL. We investigated the mechanism for this reaction focusing on roles of endocytotic internalization of ABCA1.

Methods and Results—Surface ABCA1 was labeled with biotin and traced for its internalization and degradation. ABCA1 in the cell surface was internalized within 10 minutes regardless of the presence of apoA-I. ABCA1 was intracellularly degraded and was protected against this only when exposed to extracellular apoA-I before its endocytosis. Consequently, recycle of ABCA1 to the surface was enhanced, and surface ABCA1 was increased by apoA-I. Direct inhibition of ABCA1 endocytosis led to decrease of its degradation and increase of surface ABCA1. Generation of HDL increased in parallel with surface ABCA1.

Conclusion—Surface ABCA1 is internalized and degraded, and apoA-I interferes with only the latter step to recycle ABCA1 to the surface. Increase of surface ABCA1 results in the increase of generation of HDL. (***Arterioscler Thromb Vasc Biol.* 2008;28:1820-1824**)

Key Words: ABCA1 ■ calpain ■ HDL ■ endocytosis ■ apoA-I ■ cholesterol

High density lipoprotein (HDL) is biogenerated with helical apolipoproteins and cellular lipid being mediated by the membrane protein ATP-binding cassette transporter (ABC) A1.[1] Helical apolipoprotein, mainly apolipoprotein A-I (apoA-I), is delivered and liberated by plasma HDL to somatic cells that do not synthesize apolipoproteins for biogenesis of new HDL,[2] whereas apoA-I is likely secreted from hepatocytes in a free form and interacts with its own ABCA1 in an autocrine manner.[3] HDL particles are formed with apolipoprotein and membrane phospholipid, and cholesterol is integrated into this particle being dependent on various cellular factors.[4,5] ABCA1 expression is upregulated mainly by the liver X receptor as sensing a cellular oxysterol level,[6] but it is also under the regulation by sterol regulatory element binding protein 2 in the liver perhaps to properly maintain whole body cholesterol homeostasis.[7] Interestingly, it is downregulated by activator protein 2α,[8] but its physiological role is unknown. On the other hand, ABCA1 is rapidly degraded by calpain and it seems an important regulation system for its activity of generation of HDL.[9] This proteolytic degradation is retarded when ABCA1 interacting with helical apolipoproteins[9,10] suggesting that this is a positive feedback system for HDL biogenesis. This must be a steady state ongoing in vivo in most of the cells that are chronically exposed to helical apolipoproteins such as apoA-I, although this view is yet to be proven for its relevance. It was proposed that ABCA1 is internalized by endocytosis and seems recycled,[11,12] and HDL biogenesis is associated with such endocytotic reactions.[13–16] Involvement of adaptor proteins is also suggested in the endocytosis and degradation of ABCA1.[17,18] Deletion of PEST sequence of ABCA1 inhibited its endocytosis, degradation by calpain, and HDL biogenesis, suggesting that endocytosis of ABCA1 is a key process for these all.[19] However, there are other views that HDL biogenesis takes place rather in the cell surface[20–22] than in the endosomes, where ABCA1 is entrapped. Most of these studies were carried out with ABCA1 transfected and overexpressed. In this work, we attempted to understand this complicated process by labeling the endogenous ABCA1 in cell surface and tracing it.

Materials and Methods

Cell Culture and ApoA-I

BALB/3T3 clone A31 cells were maintained and incubated in 5% Eagle minimum essential medium (MEM) with low glucose and 30% Ham F-12 (Wako) with 10% fetal calf serum (FCS) at 37°C in a humidified atmosphere of 5% CO_2.[23] THP1 cells were differentiated to macrophages by incubating in 10% FCS in the presence of 3.2×10^{-7} mol/L of phorbol 12-myristate 13-acetate (PMA; Wako)

Original received May 1, 2008; final version accepted June 25, 2008.

From Biochemistry, Nagoya City University Graduate School of Medical Sciences, Japan.

R.L. and R.A. contributed equally to this study.

Correspondence to Shinji Yokoyama at Biochemistry, Nagoya City University Graduate School of Medical Sciences, Kawasumi 1, Mizuho-cho, Mizuho-ku, Nagoya 467-8601, Japan. E-mail syokoyam@med.nagoya-cu.ac.jp

Arterioscler Thromb Vasc Biol **is available at http://atvb.ahajournals.org** **DOI: 10.1161/ATVBAHA.108.169482**

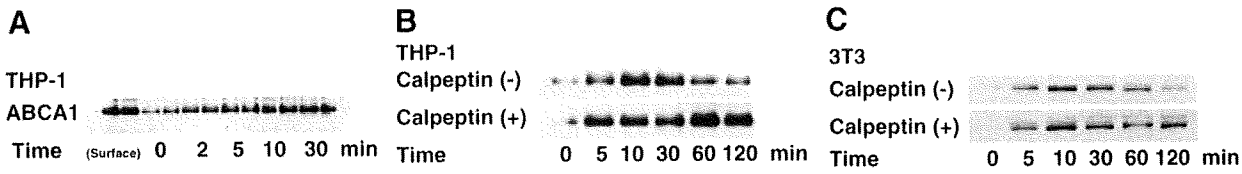

Figure 1. Internalization of ABCA1. A, Cell surface protein of the differentiated THP-1 cells was pulse-labeled with sulfo-SS-biotin. After further incubation at 37°C for the indicated time, surface biotin was cleaved to detect ABCA1 internalized. Biotinylated protein was selectively adsorbed by streptavidine-agarose and analyzed by Western blotting for ABCA1. Surface ABCA1 indicates the samples just after the biotinylation. B, Internalized-ABCA1 was detected in the presence or absence of 100 μmol/L of calpeptin in the same condition as in A. C, Internalization of ABCA1 was analyzed in BALB/3T3 cells by the same procedure as described above.

for 24 hours.[23] Human apoA-I was isolated from human plasma HDL as described previously.[24] It was used at 10 μg/mL in the medium for all the experiments unless otherwise specified.

Labeling and Tracing ABCA1

Cell surface proteins were biotinylated with sulfosuccinimidyl 2-(biotinamido)-rthyl-1, 3-dithiopropionate (sulfo-SS-biotin) (Pierce) for 1 hour at 4°C according to the methods previously reported.[25] After quenching the reaction, cells were washed and lysed, and the membrane fraction was prepared as described previously.[9] Biotinylated membrane proteins were isolated by incubating with streptavidin-agarose beads (Sigma) at 4°C for 1 hour.[26] After recovering the beads, proteins bound to the beads were eluted by incubating in the sample buffer for sodium dodecylsulfate-polyacrylamide gel electrophoresis (SDS-PAGE), and then analyzed for Western immunoblotting by using specific antibody against ABCA1 as previously described.[9] To trace the labeled surface ABCA1 for internalization, biotinylation of the cell surface proteins was cleaved by incubating the cells with 50 mmol/L reduced glutathione (Sigma) in pH 7.8 three times for 20 minutes,[26] and the remaining biotinylated ABCA1 was analyzed as above as the internalized portion. Intracellular ABCA1 degradation was measured as the time-dependent decrease of biotinylated ABCA1 after the surface biotin was cleaved after the incubation of the biotinylated cells for 1 hour at 37°C. To examine recycle of ABCA1, intracellular ABCA1 was prelabeled as above. At the various period of the incubation, the cell surface biotin was cleaved again and the remaining biotinylated ABCA1 was analyzed and compared with the biotinylated ABCA1 without the second cleavage to estimate the resurfaced ABCA1.

Cellular Lipid Release

Cellular lipid release by apoA-I was measured as described elsewhere. After incubation of the cells with apoA-I for the indicated time, concentration of cholesterol and choline-phospholipid in the medium were evaluated by enzymatic measurement.[27]

Quantification of Western Blotting Results

The bands were digitally scanned by using an EPSON GT-X700 and analyzed with Adobe Photoshop software.

Results

Figure 1A shows time-dependent internalization of ABCA1 in THP-1 cells. Most of the biotinylated ABCA1 in the surface was recovered as the internalized protein after incubating the cells at 37°C longer than 10 minutes, by cleaving the surface biotinylation with glutathione after the incubation. The internalized ABCA1 apparently decreased after 30 minutes of incubation, and this decrease was inhibited by a calpain inhibitor, calpeptin, both in THP-1 cells and BALB/3T3 cells (Figure 1B and 1C). ABCA1 was thus shown degraded by calpain after the internalization.

Degradation of ABCA1 by calpain was shown inhibited by helical apolipoproteins, such as apoA-I.[9] Therefore, the internalization of ABCA1 was examined in the presence of apoA-I. After 10 minutes of the incubation, most of the surface-labeled ABCA1 was internalized regardless of the presence of apoA-I (Figure 2A). This process was not modified any further even by the presence of calpeptin, indicating that ABCA1 was protected by apoA-I against the calpain-mediated degradation (Figure 2B). To investigate whether ABCA1 is "preprotected" by apoA-I before its internalization or extracellular apoA-I protects ABCA1 even after it is internalized, degradation of the internalized ABCA1 was examined for timing of adding apoA-I (Figure 2C). When apoA-I was present in the medium for the period before the internalization of the prebiotinylated surface ABCA1, degradation of ABCA1 was retarded (apoA-I (+)). However, when apoA-I was added to the medium after the prelabeled ABCA1 was internalized, the degradation was not much retarded (Chased). This result indicates that the protective effect of apoA-I on ABCA1 against its degradation is achieved before ABCA1 is internalized, and not by cell–apoA-I interaction to cause a distant effect on the internalized ABCA1.

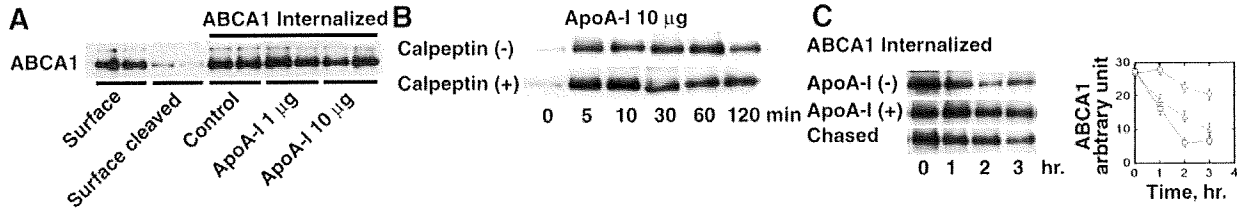

Figure 2. ABCA1 internalization and the effect of apoA-I in BALB/3T3 cells. A, ABCA1 internalization in the presence of apoA-I for 10 minutes at 37°C. "Surface" ABCA1, immediately after the labeling. "Surface cleaved", after biotin cleavage before internalization. B, ABCA1 internalization with apoA-I with and without calpeptin. C, Retardation of ABCA1 internalization by apoA-I. Cells were biotinylated and incubated for 1 hour at 37°C, and surface biotinylation was cleaved. Biotinylated ABCA1 was analyzed by Western blotting. ApoA-I (−) indicates without apoA-I throughout the incubation (squares); ApoA-I(+), with apoA-I in the preinternalization period (circles); Chased, apoA-I was added after the surface biotin cleavage (triangles).

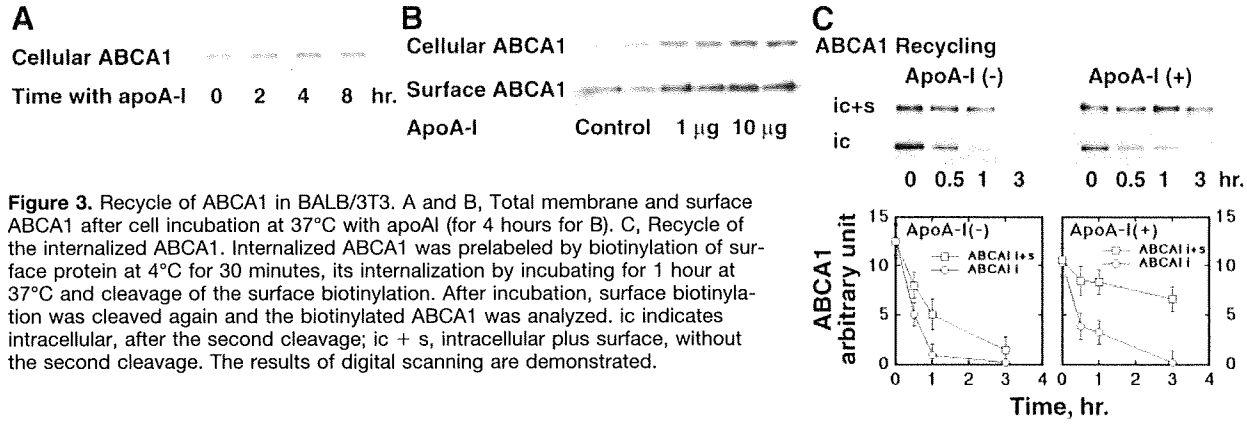

Figure 3. Recycle of ABCA1 in BALB/3T3. A and B, Total membrane and surface ABCA1 after cell incubation at 37°C with apoAI (for 4 hours for B). C, Recycle of the internalized ABCA1. Internalized ABCA1 was prelabeled by biotinylation of surface protein at 4°C for 30 minutes, its internalization by incubating for 1 hour at 37°C and cleavage of the surface biotinylation. After incubation, surface biotinylation was cleaved again and the biotinylated ABCA1 was analyzed. ic indicates intracellular, after the second cleavage; ic + s, intracellular plus surface, without the second cleavage. The results of digital scanning are demonstrated.

ABCA1 in the whole cell membrane increased up to 4 hours of the incubation, and this increase was parallel between the whole cell and cell surface (Figure 3A and 3B). To examine the mechanism for this increase of the surface ABCA1, recycle to the surface of the internalized ABCA1 was examined. After the prelabeled ABCA1 was internalized and surface biotinylation was cleaved, the cells were further incubated for certain periods of time and the surface biotinylation was cleaved again to assess the recycled ABCA1 to the surface (Figure 3C). In the absence of apoA-I, the internalized ABCA1 rapidly disappeared, and only its small portion was found recycled to the surface. In the presence of apoA-I, clearance of the internalized ABCA1 was substantially retarded as presented above, and a large portion of it was found recycled to the surface. Thus, apoA-I increased recycling of ABCA1 apparently by blocking the intracellular calpain-mediated degradation.

To examine whether internalization of ABCA1 is mandatory for the HDL biogenesis reaction, clathrin-mediated endocytosis was inhibited by cytochalasin D.[28,29] ABCA1 in the cell was decreased within 60 minutes in the absence of helical apolipoproteins when its synthesis was inhibited by cycloheximide (Figure 4A). When the endocytosis was inhibited by cytochalasin D, ABCA1 did not decrease. The increase of cellular ABCA1 by cytochalasin D was shown attributable to its increase in the cell surface (Figure 4B) as its endocytosis was strongly inhibited (Figure 4C).

Finally, generation of HDL was evaluated by measuring release of cellular phospholipid and cholesterol by apoA-I[5,30] when the endocytosis of ABCA1 was inhibited and its amount in the cell surface was increased. As shown in Figure 5, releases of phospholipid and cholesterol were both increased by this treatment. As apoA-I by itself increases surface ABCA1 by increasing its recycling, the increment of the HDL biogenesis should not be to the same extent as the increase of surface ABCA1 by cytochalasin D in the absence of apoA-I. This was in fact demonstrated in Figure 5B. The relative increase of the surface ABCA1 by cytochalasin D was to a less extent in the presence of apoA-I because the surface ABCA1 is already increased by apoA-I even in the absence of cytochalasin D. The increase of ABCA1 by cytochalasin D in the presence of apoA-I was parallel to the increase of lipid release by apoA-I (Figure 5C).

Discussion

In summary, we have shown that: (1) ABCA1 is rapidly degraded intracellularly by calpain after its clathrin-mediated endocytotic internalization in the absence of helical apolipoprotein; (2) Helical apolipoproteins, represented by apoA-I, protect ABCA1 from the degradation, not by inhibiting the internalization but by inhibiting the intracellular proteolysis; (3) This inhibition is achieved by preexposure of ABCA1 to extracellular apoA-I before the internalization and not by the exposure of the cells after ABCA1 is internalized;

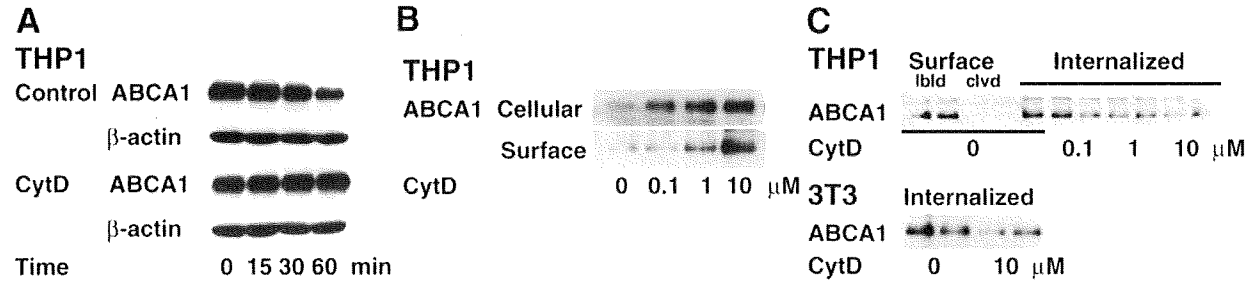

Figure 4. Effects of cytochalasin D on ABCA1 in differentiated THP-1 cells. A, Cells were incubated with 10 μmol/L cytochalasin D at 37°C and total membrane ABCA1 was analyzed. B, ABCA1 in total membrane and cell surface after incubation with cytochalasin D at 37°C for 30 minutes. C, ABCA1 internalization in the presence of cytochalasin D. Surface lbld indicates the biotinylated ABCA1 immediately after the labeling; Surface clvd, biotinylated ABCA1 after cleavage of surface biotin before the incubation at 37°C; Internalized, ABCA1 after the incubation at 37°C for 10 minutes and cleavage of the surface biotin. ABCA1 in BALB/3T3 cells were also analyzed for the internalization by the incubation for 10 minutes at 37°C.

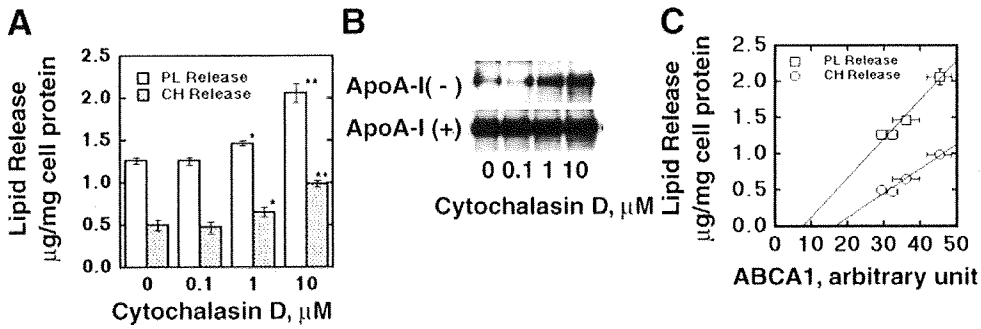

Figure 5. Effect of cytochalasin D on the apoAI-mediated HDL biogenesis. A, Differentiated THP-1 cells were incubated with apoA-I for 6 hours, and release of cholesterol and phospholipids was measured. The effect of cytochalasin D was examined in a dose-dependent manner. The data represent mean± SE for 3 measurements as $^{*}P<0.05$ and $^{**}P<0.01$ from the control. B, ABCA1 protein in cell surface in the absence and presence of apoA-I for 6 hours. C, The results of B were digitally scanned, and the lipid release data were plotted against the surface ABCA1.

(4) ABCA1 that escaped from the intracellular proteolysis is recycled to the cell surface, and apoA-I therefore enhances this process to increase cell surface ABCA1; (5) Generation of HDL is directly proportional to the surface ABCA1 level. The results are summarized in supplemental Figure I (available online at http://atvb.ahajournals.org).

It is well recognized that activity of ABCA1 is a rate-limiting factor for biogenesis of HDL and therefore plasma HDL concentration in vivo.[1] Expression of the gene has been shown to regulate it in vitro and in vivo,[6–8] but the degradation of ABCA1 protein seems an important regulatory factor for its activity as a posttranslational regulation at the cellular level,[9,10] whose physiological relevance, however, is yet to be proven.

We used THP-1 cells and BALB/3T3 fibroblasts as models for generation of HDL. HDL biogenesis in vivo is largely in the liver and intestine,[31] but any peripheral cells must carry on the HDL biogenesis reaction for their cholesterol homeostasis.[1] Indeed, it was proposed that peripheral tissue may be a significant source of plasma HDL in human.[32] Therefore, the use of these cells is justified to investigate mechanism for HDL biogenesis by the ABCA1/apolipoprotein system. ABCA1 seems stabilized in hepatocytes in an autocrine mechanism by a large amount of apoA-I produced and secreted by themselves, and the effects of additional apoA-I may not be apparent.[3]

When HDL generation is ongoing, helical apolipoproteins interact with ABCA1 before its internalization and make ABCA1 resistant to the calpain-mediated degradation. Consequently, a large portion of ABCA1 is recycled to the surface without degradation for further HDL generation. This view is consistent with most of the previous findings that apoA-I/ABCA1 complex recycles and apoA-I may be released by exocytosis during the HDL generation reactions.[11,12] Most of the cells in the body are chronically exposed to HDL, which liberates apoA-I for generation of HDL.[2] Therefore, in the physiological environment in vivo, ABCA1 seems protected from the degradation and its clearance rate should be rather slow. Recently, 2 independent articles proposed that HDL biogenesis by ABCA1 mainly takes place on cell surface rather than in the endosomes by tracing the labeled apoA-I in the presence of transfected ABCA1.[21,22] The conclusion in the present work is consistent with these proposals and may not agree with the view that HDL biogenesis occurs intracellularly.[13–16]

In the steady state of HDL generation, ABCA1 should be increased in cell surface from the baseline condition without apolipoprotein. It is therefore of interest whether there is a room for further increase of surface ABCA1 and consequently for the increase of HDL biogenesis by inhibiting the endocytotic internalization of ABCA1. Inhibition of the endocytosis by cytochalasin D increased surface ABCA1×50 to 60% as well as HDL biogenesis in parallel (Figure 5C).

Sources of Funding

This works was supported in part by Grants-in-aids from Ministry of Education, Culture and Sports, Science and Technology of Japan, and from Japan Health Science Foundation/Ministry of Health, Labor and Welfare of Japan, and by the Program for the Promotion of Fundamental Studies in Health Sciences of the National Institute of Biomedical Innovation of Japan.

Disclosures

Shinji Yokoyama is involved in establishment of a Venture Company, HYKES Laboratories.

References

1. Yokoyama S. Assembly of high-density lipoprotein. *Arterioscler Thromb Vasc Biol.* 2006;26:20–27.
2. Okuhira K, Tsujita M, Yamauchi Y, Abe-Dohmae S, Kato K, Handa T, Yokoyama S. Potential involvement of dissociated apoA-I in the ABCA1-dependent cellular lipid release by HDL. *J Lipid Res.* 2004;45:645–652.
3. Tsujita M, Wu CA, Abe-Dohmae S, Usui S, Okazaki M, Yokoyama S. On the hepatic mechanism of HDL assembly by the ABCA1/apoA-I pathway. *J Lipid Res.* 2005;46:154–162.
4. Yamauchi Y, Abe-Dohmae S, Yokoyama S. Differential regulation of apolipoprotein A-I/ATP binding cassette transporter A1-mediated cholesterol and phospholipid release. *Biochim Biophys Acta.* 2002; 1585:1–10.
5. Hayashi M, Abe-Dohmae S, Okazaki M, Ueda K, Yokoyama S. Heterogeneity of high density lipoprotein generated by ABCA1 and ABCA7. *J Lipid Res.* 2005;46:1703–1711.
6. Venkateswaran A, Laffitte BA, Joseph SB, Mak PA, Wilpitz DC, Edwards PA, Tontonoz P. Control of cellular cholesterol efflux by the nuclear oxysterol receptor LXR alpha. *Proc Natl Acad Sci U S A.* 2000; 97:12097–12102.
7. Tamehiro N, Shigemoto-Mogami Y, Kakeya T, Okuhira K, Suzuki K, Sato R, Nagao T, Nishimaki-Mogami T. Sterol regulatory element-binding protein-2- and liver X receptor-driven dual promoter regulation of hepatic ABC transporter A1 gene expression: mechanism underlying the unique response to cellular cholesterol status. *J Biol Chem.* 2007;282: 21090–21099.
8. Iwamoto N, Abe-Dohmae S, Ayaori M, Tanaka N, Kusuhara M, Ohsuzu F, Yokoyama S. ATP-binding cassette transporter A1 gene transcription is downregulated by activator protein 2alpha. Doxazosin inhibits activator

protein 2alpha and increases high-density lipoprotein biogenesis independent of alpha1-adrenoceptor blockade. *Circ Res.* 2007;101:156–165.
9. Arakawa R, Yokoyama S. Helical apolipoproteins stabilize ATP-binding cassette transporter A1 by protecting it from thiol protease-mediated degradation. *J Biol Chem.* 2002;277:22426–22429.
10. Arakawa R, Hayashi M, Remaley AT, Brewer BH Jr, Yamauchi Y, Yokoyama S. Phosphorylation and stabilization of ATP binding cassette transporter A1 by synthetic amphiphilic helical peptides. *J Biol Chem.* 2004;279:6217–6220.
11. Neufeld EB, Remaley AT, Demosky SJ, Stonik JA, Cooney AM, Comly M, Dwyer NK, Zhang M, Blanchette-Mackie J, Santamarina-Fojo S, Brewer HB Jr. Cellular localization and trafficking of the human ABCA1 transporter. *J Biol Chem.* 2001;276:27584–27590.
12. Neufeld EB, Stonik JA, Demosky SJ Jr, Knapper CL, Combs CA, Cooney A, Comly M, Dwyer N, Blanchette-Mackie J, Remaley AT, Santamarina-Fojo S, Brewer HB Jr. The ABCA1 transporter modulates late endocytic trafficking: insights from the correction of the genetic defect in Tangier disease. *J Biol Chem.* 2004;279:15571–15578.
13. Takahashi Y, Smith JD. Cholesterol efflux to apolipoprotein AI involves endocytosis and resecretion in a calcium-dependent pathway. *Proc Natl Acad Sci U S A.* 1999;96:11358–11363.
14. Chen W, Sun Y, Welch C, Gorelik A, Leventhal AR, Tabas I, Tall AR. Preferential ATP-binding cassette transporter A1-mediated cholesterol efflux from late endosomes/lysosomes. *J Biol Chem.* 2001;276:43564–43569.
15. Smith JD, Waelde C, Horwitz A, Zheng P. Evaluation of the role of phosphatidylserine translocase activity in ABCA1-mediated lipid efflux. *J Biol Chem.* 2002;277:17797–17803.
16. Hassan HH, Bailey D, Lee DY, Iatan I, Hafiane A, Ruel I, Krimbou L, Genest J. Quantitative analysis of ABCA1-dependent compartmentalization and trafficking of apolipoprotein A-I: Implications for determining cellular kinetics of nascent HDL biogenesis. *J Biol Chem.* 2008;283:11164–11175.
17. Munehira Y, Ohnishi T, Kawamoto S, Furuya A, Shitara K, Imamura M, Yokota T, Takeda S, Amachi T, Matsuo M, Kioka N, Ueda K. a1-syntrophin modulates turnover of ABCA1. *J Biol Chem.* 2004;279:15091–15095.
18. Okuhira K, Fitzgerald ML, Sarracino DA, Manning JJ, Bell SA, Goss JL, Freeman MW. Purification of ATP-binding cassette transporter A1 and associated binding proteins reveals the importance of beta1-syntrophin in cholesterol efflux. *J Biol Chem.* 2005;280:39653–39664.
19. Chen W, Wang N, Tall AR. A PEST deletion mutant of ABCA1 shows impaired identification and defective cholesterol efflux from late endosomes. *J Biol Chem.* 2005;280:29277–29281.
20. Witting SR, Maiorano JN, Davidson WS. Ceramide enhances cholesterol efflux to apolipoprotein A-I by increasing the cell surface presence of ATP-binding cassette transporter A1. *J Biol Chem.* 2003;278:40121–40127.
21. Faulkner LE, Panagotopulos SE, Johnson JD, Woollett LA, Hui DY, Witting SR, Maiorano JN, Davidson WS. An analysis of the role of a retroendocytosis pathway in ATP-binding cassette transporter (ABCA1) - mediated cholesterol efflux from macrophages. *J Lipid Res.* 2008;49:1322–1332.
22. Denis M, Landry YD, Aha X. ATP-binding cassette A1-mediated lipidation of apolipoprotein A-I occurs at the plasma membrane and not in the endocytotic compartment. *J Biol Chem.* 2008;283:16178–16186.
23. Arakawa R, Tamehiro N, Nishimaki-Mogami T, Ueda K, Yokoyama S Fenofibric acid, an active form of fenofibrate, increases apolipoprotein A-I-mediated high-density lipoprotein biogenesis by enhancing transcription of ATP-binding cassette transporter A1 gene in a liver X receptor-dependent manner. *Arterioscler Thromb Vasc Biol.* 2005;25:1193–1197.
24. Yokoyama S, Tajima S, Yamamoto A. The process of dissolving apolipoprotein A-I in an aqueous buffer. *J Biochem (Tokyo).* 1982;91:1267–1272.
25. von Boxberg Y, Wütz R, Schwarz U. Use of the biotin-avidin system for labelling, isolation and characterization of neural cell-surface proteins. *Eur J Biochem.* 1990;190:249–256.
26. Vagin O, Turdikulova S, Yakubov I, Sachs G. Use of the H,K-ATPase beta subunit to identify multiple sorting pathways for plasma membrane delivery in polarized cells. *J Biol Chem.* 2005;280:14741–14754.
27. Abe-Dohmae S, Suzuki S, Wada Y, Aburatani H, Vance DE, Yokoyama S. Characterization of apolipoprotein-mediated HDL generation induced by cAMP in a murine macrophage cell line. *Biochemistry.* 2000;39:11092–11099.
28. Jackman MR, Shurety W, Ellis JA, Luzio JP. Inhibition of apical but not basolateral endocytosis of ricin and folate in Caco-2 cells by cytochalasin D. *J Cell Sci.* 1994;107: 2547–2556.
29. Szaszi K, Paulsen A, Szabo EZ, Numata M, Grinstein S, Orlowski J. Clathrin-mediated endocytosis and recycling of the neuron-specific Na+/H+ exchanger NHE5 isoform. Regulation by phosphatidylinositol 3′-kinase and the actin cytoskeleton. *J Biol Chem.* 2002;277:42623–42632.
30. Hara H, Yokoyama S. Interaction of free apolipoproteins with macrophages. Formation of high density lipoprotein-like lipoproteins and reduction of cellular cholesterol. *J Biol Chem.* 1991;266:3080–3086.
31. Timmins JM, Lee JY, Boudyguina E, Kluckman KD, Brunham LR, Mulya A, Gebre AK, Coutinho JM, Colvin PL, Smith TL, Hayden MR, Maeda N, Parks JS. Targeted inactivation of hepatic Abca1 causes profound hypoalphalipoproteinemia and kidney hypercatabolism of apoA-I. *J Clin Invest.* 2005;115:1333–1342.
32. Nanjee MN, Cooke CJ, Olszewski WL, Miller NE. Lipid and apolipoprotein concentrations in prenodal leg lymph of fasted humans. Associations with plasma concentrations in normal subjects, lipoprotein lipase deficiency, and LCAT deficiency. *J Lipid Res.* 2000;41:1317–1327.

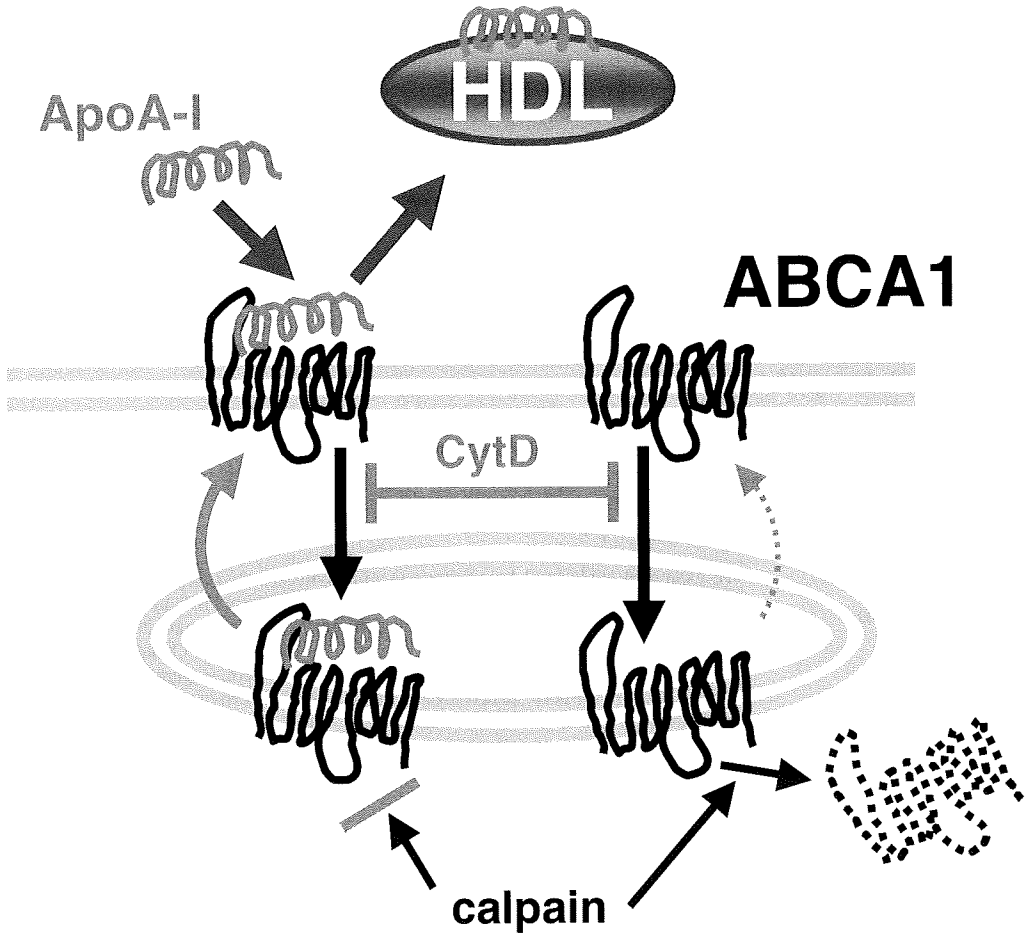

Supplementary Figure I. Schematic summary of the results. In the absence of apoA-I (right), ABCA1 is internalized and degraded by calpain and only very limited amount of ABCA1 could be recycled to the surface. Inhibition of calpain may lead to more recycle of ABCA1 to the surface. In the presence of apoA-I (left), ABCA1 is pre-protected by apoA-I in the surface against the intracellular calpain-mediated proteolysis. ABCA1 is therefore recycled to the surface. Inhibition of ABCA1 internalization by cytochalasin D (CytD) results in the increase of surface ABCA1. Surface ABCA1 is parallel to generation of HDL by apoA-I.

Biochimica et Biophysica Acta 1791 (2009) 1197–1205

Contents lists available at ScienceDirect

Biochimica et Biophysica Acta

journal homepage: www.elsevier.com/locate/bbalip

Cholesterol homeostasis in ABCA1/LCAT double-deficient mouse

Mohammad Anwar Hossain [a,1], Maki Tsujita [a], Nobukatsu Akita [a,b], Fumihiko Kobayashi [a], Shinji Yokoyama [a,*]

[a] Biochemistry, Nagoya City University Graduate school of Medical Sciences, Kawasumi 1, Mizuho-cho, Mizuho-ku, Nagoya 467-8601, Japan
[b] Cardio-Renal Medicine and Hypertension, Nagoya City University Graduate school of Medical Sciences, Nagoya 467-8601, Japan

ARTICLE INFO

Article history:
Received 31 May 2009
Received in revised form 7 August 2009
Accepted 24 August 2009
Available online 1 September 2009

Keywords:
Cholesterol
HDL
ABCA1
LCAT
Atherosclerosis

ABSTRACT

We examined cholesterol homeostasis in mice with the two major cholesterol transport pathways for catabolism interrupted by disrupting *abca1*, *lcat*, or both. Plasma HDL markedly decreased in these genotype but LDL/VLDL decreased only in the double deficiency. Fractional catabolic rate of HDL increased in the order of wild type<*abca1*(−/−)=*lcat*(−/−)<*abca1*(−/−)*lcat*(−/−). Cholesterol accumulated in the liver by disrupting either gene and more by the double disruption. HDL biogenesis by primary-cultured hepatocytes was negligible in the *abca1* deficiency and substantially reduced in the *lcat* deficiency. Secretion of LDL/VLDL was also decreased in these cells but to a less extent. Cholesterol content in the hepatocytes was in a reciprocal order to lipoprotein generation. Expression of hepatic mRNA of the sterol-related genes reflected the cellular cholesterol increase, such as decrease in SREBP2 and HMG-CoA reductase and increase in apoA-I, apoE, and ABCG1. Cholesterol decreased in the steroidogenic organs by disruption of either gene resulting from low-plasma HDL. Cholesterol in other peripheral tissues generally decreased under normal chow feeding, and interestingly, it was recovered by high-cholesterol feeding, including the cholesterol content in the brain. No apparent vascular lipid deposition was observed in any genotype. Deletion of the two major factors in "reverse cholesterol transport" may not directly result in severe cholesterol transport stagnation in the body of mouse. Other compensatory pathways may back up cholesterol transport among the organs and tissues even when these pathways are impaired.

1. Introduction

Cholesterol, an essential constituent for animal cell membrane and a precursor of steroid hormones, is not catabolized in peripheral tissues. Except for generation of steroid hormones in a very limited amount in the specified organs, most of the body cholesterol molecules are converted to bile acids in the liver for excretion. Therefore, cholesterol is released from somatic cells and transported to the liver in order to maintain its homeostasis at the levels of cells and whole body. Plasma HDL is thought to play a central role in this transport system. HDL particles are mainly generated in the liver by the interaction of the locally generated helical apolipoprotein such as apoA-I with the membrane protein ATP-binding cassette transporter (ABC) A1 removing cellular phospholipid and cholesterol [1]. In peripheral tissues, apoA-I carried by HDL dissociates from the particles and interacts with ABCA1 in the cell surface to generate HDL with the cellular lipid [2]. HDL particles also receive cellular cholesterol molecules released by diffusion. The latter reaction is facilitated by acyl-esterificaiton of cholesterol in the HDL particles by lecithin, cholesterol acyltransferase (LCAT) [3], and by the presence of ABCG1 in the cell membrane [4].

Plasma HDL concentration inversely correlates with a risk of atherosclerotic clinical events such as coronary heart diseases and is considered as a strong "negative" risk factor for atherosclerosis [5]. It is believed that this is strongly associated with the above mentioned function of HDL in transporting cholesterol from the peripheral tissues to the liver. HDL indeed removes cholesterol accumulated in the cells in vitro [6].

As mentioned above, two independent mechanisms [7] are working for the release of cellular cholesterol. One is a nonspecific aqueous diffusion of cholesterol molecules between the cell membrane and HDL particles in which cholesterol acyl-esterification on HDL generates a gradient of unesterified cholesterol for its continuous outflow from the cell surface to HDL [3]. The presence of ABCG1 in the cell membrane may also facilitate the release of cell cholesterol in this pathway [4]. The other pathway is mediated by a direct interaction of lipid-free apolipoproteins with cell surface to generate new disc-like HDL particles by removing cellular phospholipid and cholesterol [8]. This pathway requires a specific membrane protein ABCA1 as a functional interaction site for apolipoproteins [9–11] and subsequent linkage of the ABCA1/apolipoprotein interaction to the regulation of cholesterol trafficking from the intracellular pool to a membrane domain used for the HDL assembly [12].

* Corresponding author. Tel.: +81 52 853 8139; fax: +81 52 841 3480.
E-mail address: syokoyam@med.nagoya-cu.ac.jp (S. Yokoyama).
[1] Present address: St. Paul's Hospital, Vancouver, British Columbia, Canada V6Z 1Y6.

1388-1981/$ – see front matter © 2009 Elsevier B.V. All rights reserved.
doi:10.1016/j.bbalip.2009.08.009

The hypolipidemic drug probucol is known to reduce plasma HDL. This drug has been shown to inhibit ABCA1 [13,14] and exhibited a phenotype similar to Tangier disease, a genetic deficiency of ABCA1, in mice [15]. We used probucol in LCAT-deficient mice to attempt inhibition of both ABCA1 and LCAT, the two major players in cholesterol transport from the tissues to the liver [16]. This model showed that inhibition of the two pathways did not cause massive systemic cholesterol accumulation. However, cholesterol content in the liver significantly increased when both pathways were inhibited, indicating that the liver is a major source of HDL in mice. However, probucol is known to have various puzzling effects on lipid and lipoprotein metabolism and anti-atherogenic natures [17], some of which may be attributed to its strong anti-oxidative potential [18]. We therefore undertook more specific approach to demonstrate the effects of inhibition of LCAT and ABCA1 by generating double knock-out mouse of these genes.

2. Methods

2.1. Experimental animals

The C57BL/6 mice were obtained from a local animal supplier. *Abca1*-deficient heterozygote (DBA/1-*abca1*tm1Jdm/J) mice were purchased from Jackson's Animal Laboratories (Stony Brook, NY) and bred to have the C57BL/6N genetic background [1]. The *lcat* (−/−) mice were kindly provided by Dr. E. Rubin at Laurence Berkeley Laboratory (Berkeley, Calif) [19]. The C57BL/6 mice with six different genotypes, *abca1*(+/+)*lcat*(+/+) (wild type), *abca1*(+/−)*lcat*(+/+), *abca1*(−/−)*lcat*(+/+), *abca1*(+/+)*lcat*(−/−), *abca1*(+/−)*lcat*(−/−), and *lcat*(−/−)*abca1*(−/−), were developed through breeding of the *lcat*(+/−) and *abca1*(+/−) mice at the Center for Experimental Animal Science, Nagoya City University Graduate School of Medical Sciences. The newborn mice were weaned and sexually segregated at the 3 weeks. The genotype of mice was identified at the 5th week by the multiplex polymerase chain reaction genotype analysis of the tail genomic DNA. For detecting *lcat* genotypes, the forward primers either hybridize specificity to the neo-resistant gene (5′-AAC GAG ATC AGC AGC CTC TGT TCC AC-3′) or to the targeted region (5′-TGA ACT CAG TAA CCA CAG ACG GCC TG-3′) and share a common reverse primer that hybridizes to the *lcat* gene (5′-GTC CTC TGT CTT ACG GTA GCA CAT CC-3′). *Abca1* genotypes were detected according to the methods previously described [1]. The animals with each genotype ($n=4$) of 20–24 weeks old were fed with normal chow containing 0.2% cholesterol or with high-cholesterol chow containing 1.2% cholesterol for 2 weeks. All the parameters were measured at the end of the feeding term. All the experimental protocols including these animals have been prepared according to the institutional guideline and approved by the institutional experimental animal welfare committee (approval number H17-15).

2.2. Primary hepatocytes cell culture

Hepatocytes were isolated from the mouse liver according to the EDTA-collagenase two-step perfusion method and were used in primary culture at a concentration of 0.2×10^6 cells/mL in a collagen coated plate in the presence of Dulbecco's modified Eagle medium (MEM) containing 4.5 g/L glucose [1,20]. The cells were incubated in MEM-alpha containing 0.02% (wt./vol.) bovine serum albumin (BSA) for 16 to 18 hours, and the culture medium was analyzed for lipoprotein and the cells were used for the analysis of mRNA and proteins. HDL and LDL/VLDL fractions of the medium were obtained as the density fractions of 1.063–1.21 g/ml and below 1.063 g/ml, respectively, by ultracentrifugation in a himac CP80β by using a P50AT4 rotor at 49,000 rpm for 16 hours at 4 °C. Lipid was extracted from each lipoprotein fraction with four volumes of chloroform/methanol (2:1, vol./vol.) overnight, and the organic layer was used for the determination of cholesterol and choline phospholipid by colorimetric enzymatic assay system (Kyowa Medics, Japan).

2.3. HPLC analysis of mouse plasma lipoprotein

Blood was collected from the mouse tail and 100 μl of the plasma was analyzed for lipoprotein profile by high-performance liquid chromatography (HPLC) using a size exclusion column, TSK gel G3000SW (7.5 mm internal diameter × 60.0 cm length) in phosphate-buffered saline (PBS) at a flow rate of 0.33 mL/min [16,21]. The eluted solution was fractionated by every 330 μL. For each fraction, concentrations of total cholesterol and choline phospholipid were determined by colorimetric enzymatic assay systems (Kyowa Medics, Japan) and protein content was assayed.

2.4. Tissue cholesterol analysis and histochemical analysis

Mice were anesthetized and underwent euthanasia by exsanguinations with cardiac puncture. The animal's whole body was perfused with PBS and then with PBS containing 4% paraformaldehyde by infusing into the left ventricle and cutting the right atrium of the heart. The liver, adrenal gland, ovary (female), testis (male), brain, kidney, lungs, heart, thymus, and spleen were collected from each animal. For tissue cholesterol analysis, the organs were mechanically homogenized, and the content of free and esterified cholesterol were determined by enzymatic methods (Kyowa Medics, Japan) after lipid extraction with four volumes of chloroform/methanol (2:1, vol./vol.) overnight [16]. For the histochemical analysis of vascular lipid deposit, cardiac atrium and valves were collected from the cholesterol-fed animals. Aortic valve region was frozen in OCT compound and sliced with a cryostat (Leica CM3050S; 12 μm). The frozen sections were washed three times with PBS and stained with Oil red O. Tissues were observed in a Biozero microscope system BZ8000 (Keyence Japan).

2.5. Western blotting analysis of protein

ABCA1 protein in the liver was analyzed by Western blotting [20]. The liver was homogenized with a hypotonic solution 50 mM Tris–HCl buffer (pH 7.4) containing protease inhibitors. The homogenized protein, 60 μg, was dissolved in 9 M urea, 2% Triton X-100, and 1% dithiothreitol, and analyzed by 6% polyacrylamide electrophoresis for Western blotting by using specific antibodies against ABCA1 and Bip/GRP78.

2.6. Catabolic rate of HDL in mouse plasma

Clearance rate of HDL lipid was measured as previously described [15]. HDL was labeled with [22] cholesteryl oleoyl ether by incubating the mouse (C57BL/6) plasma, 5 mL, at 37 °C for 48 hours with 10 mg of egg yolk phosphatidylcholine sonicated vesicle containing 1 mCi of the labeled cholesteryl ether oleate and lipoprotein-free human plasma, 10 mg. This mixture also contained an LCAT inhibitor 5,5′-dithiobis (2-nitrobenzoic acid) (48% wt./vol.), trasylol (0.25% vol./vol.), gentamicin (0.125% vol./vol.), 10% NaN_3 (1.25% vol./vol.), 0.5 M EDTA (0.125% vol./vol.). The mixture was adjusted to a density of $d<1.063$ g/mL with NaBr and ultracentrifuged at 49,000 rpm for 24 hours to remove VLDL/LDL. The HDL fraction was isolated by further ultracentrifugation at a density of 1.21 g/mL for 48 hours. The labeled HDL was thoroughly dialyzed against PBS. The specific radioactivity of the HDL was 1.6×10^5 dpm/μg of cholesterol moiety in cholesteryl ester (CE). The labeled HDL of 100 μL (containing 8 μg CE and 1.3×10^6 dpm) was injected into the mouse tail caudal vein. The blood, 30 μL, was collected from the caudal vein on the other side into a microtube containing 0.02 mM EDTA every 30 minutes after injection for 3 hours for counting the radioactivity using a scintillation counter. The HDL fraction was isolated from the plasma collected at 3 hours by ultracentrifugation and measured for protein and CE by

Table 1
Plasma lipoprotein lipids of mice under feeding of low cholesterol chow and high cholesterol chow.

	Genotype	Low cholesterol chaw (0.2 %)						High cholesterol chaw (1.2 %)					
		Male			Female			Male			Female		
		TC	FC	PL	TC	FC	PL	TC	FC	PL	TC	FC	PL
HDL	*abca1(+/+)lcat(+/+)*	51.7±4.0	25.4±3.3	141.3±42.6	41.1±12.8	27.9±7.1	127.2±26.0	62.5±6.3	52.2±2.9	206±27.5	65.9±9.8	55.7±9.4	192.8±30.6
	abca1(+/-)lcat(+/+)	32.8±3.9*	9.6±4.7**	116.3±40.2	15.9±4.6*	10.0±2.3**	73.37±4.0	33.3±12.0	23.0±0.8*	131.9±6.0**	27.5±7.6*	20.0±0.2**	71.9±13.0*
	abca1(-/-)lcat(+/+)	12.0±0.6**	5.8±0.2**	40.6±3.5*	3.6±1.5**	3.4±1.9**	30.0±0.5**	13.0±0.7**	6.1±0.3**	38.8±6.6**	17.2±9.0**	9.7±3.5**	36.9±6.4**
	abca1(+/+)lcat(-/-)	5.9±3.0**	6.0±0.3**	29.5±13.2*	4.1±1.3**	4.2±1.5**	32.0±0.7**	12.0±5.1**	11.0±3.6**	64.3±8.6**	11.0±0.3**	12.6±2.0**	31.8±7.3**
	abca1(+/-)lcat(-/-)	14.0±6.3**	12.0±7.5**	34.0±21.0*	6.5±0.7**	6.0±2.6**	35.0±2.1**	11.0±2.3**	11.0±4.2**	36.7±5.7**	8.28±2.0**	7.5±3.0**	59.2±2.5**
	abca1(-/-)lcat(-/-)	2.8±0.3**	3.1±0.2**	13.2±0.9**	3.8±1.1**	4.0±2.9**	13.0±1.2**	3.7±1.9**	3.0±0.2**	30.0±0.0**	5.1±0.4**	4.6±2.5**	28.7±7.2**
LDL/VLDL	*abca1(+/+)lcat(+/+)*	13.4±2.5	10.3±3.0	51.2±15.4	20.0±7.7	13.0±3.6	48.0±13.9	31.0±9.2	25.8±5.1	94.8±41.4	13.7±0.6	11.7±6.8	68.0±6.5
	abca1(+/-)lcat(+/+)	13.8±2.8	5.8±2.6	42.0±11.1	17.3±7.9	15.0±5.0	60.0±27.6	28.8±12.9	23.0±4.5	99.8±33.9	21.6±2.0**	14.4±2.0	75.4±6.9
	abca1(-/-)lcat(+/+)	11.8±0.4	11.1±2.8	41.9±4.8	9.0±2.5	8.5±8.7	41.0±12.6	22.7±8.1	20.1±4.0	64.5±4.4	17.8±2.8	10.1±7.7	73.0±2.5
	abca1(+/+)lcat(-/-)	15.9±8.4	16.1±5.6	79.4±30.1	16.9±4.5	15.2±7.3	79.8±4.5*	27.9±14.9	24.1±0.1	67.8±16.3	19.4±0.4	19.8±19.8	68.9±5.3
	abca1(+/-)lcat(-/-)	18.2±11.0	22.6±5.5	63.6±27.3	17.9±5.1	16.0±3.8	93.0±18.2*	18.6±8.2	19.6±4.0	63.7±12.5	14.0±0.3**	18.0±6.2	59.8±14.2
	abca1(-/-)lcat(-/-)	8.3±0.1*	8.9±3.5*	42.2±1.7	6.7±1.7*	3.8±2.8**	33.2±6.5	19.8±7.9	19.4±12.6	66.6±20.4	4.9±0.7**	5.6±2.1	68.4±16.0

Blood plasma obtained from the male and female mice having the genotypes indicated was separated by ultracentrifugation for HDL and LDL/VLDL reactions ($d = 1.21 - 1.063$, and $d > 1.063$) and total cholesterol (TC), free (unesterified) cholesterol (FC) and phospholipid (PL) were determined for each fraction.

colorimetric enzymatic assay (Kyowa Medics, Japan) to calculate the specific radioactivity activity of CE in plasma. The liver, small intestine, kidney, ovary, and adrenal glands were homogenized, and the radioactivity in each tissue was counted per 100 μg protein.

2.7. RNA extraction and real-time quantitative polymerase chain reaction (PCR)

Total RNA was extracted from the mouse liver by using RNA extraction reagent (Isogen, Nippon Gene). Single-strand cDNA was synthesized by a SuperScript™ pre-amplification system (Invitrogen) from 5 μg of the total RNA. PCR was carried out for the cDNA by using primers (sense and antisense) of mouse ABCA1 (5′-CTC AGA GGT GGC

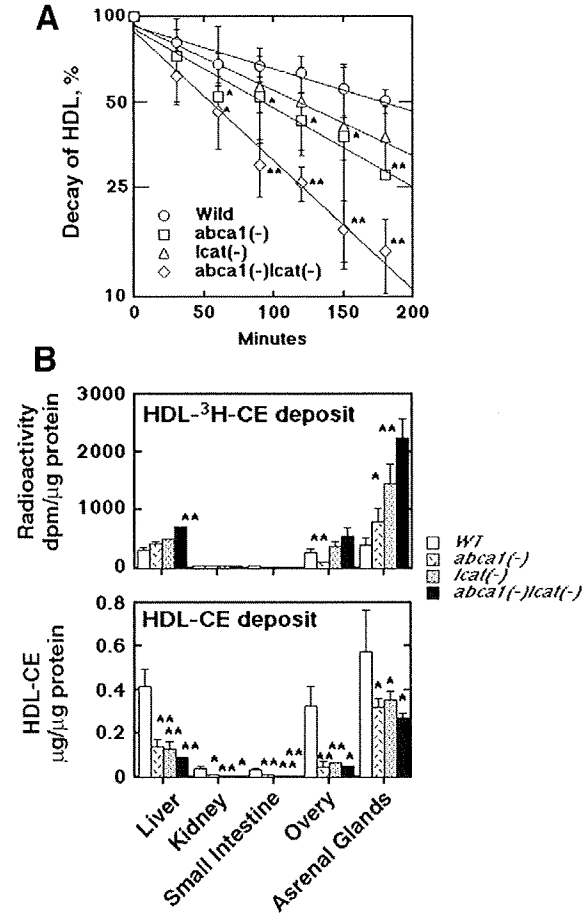

Fig. 1. Plasma clearance and tissue deposit of HDL cholesteryl ester. HDL of mouse (C57BL/6) plasma was labeled with [^{3}H]cholesteryl ether oleate and injected into the tail caudal vain of the mice with the four genotype of *abca1(+/+)lcat(+/+)* (wild), *abca1(−/−)lcat(+/+)* (*abca1(−)*), *abca1(+/+)lcat(−/−)* (*lcat(−)*), and *abca1(−/−)lcat(−/−)* (*abca1(−)lcat(−)*) ($n = 3$ for each), fed with normal chow. (A) Blood was taken with the 30-minute interval for 3 hours to measure the decay of the radioactivity. The data are plotted in a semilogarithmic manner and fit by exponential curves by the least square regression assuming that the decay follows first-order kinetics. Each data point represents the mean ± SD after the count was standardized for the level at 0 minutes as 100%. First-order constants were as follows: -1.52×10^{-3}, -2.82×10^{-3}, -2.33×10^{-3}, and -4.61×10^{-3} min^{-1} for *abca1(+/+)lcat(+/+)*, *abca1(−/−)lcat(+/+)*, *abca1(+/+)lcat(−/−)*, and *abca1(−/−)lcat(−/−)*, respectively. (B) Deposit of [^{3}H]cholesteryl ether (upper panel) and that of CE mass from HDL (lower panel). The latter data were calculated from specific activity of [^{3}H]cholesteryl ether/HDL-CE in the plasma at the zero time for each mouse. Liver, kidney, small intestine, ovary, and adrenal glands were collected at 3 hours after the injections described in the text. Organs were mechanically homogenized and 100 mg protein was used for counting [^{3}H]cholesteryl ether in a scintillation counter. The values represent mean ± SD for three determinations (*$p<0.05$, **$p<0.01$ from wild type).

TCT GAT GAC-3′ and 5′-CCC ATA CAG CAA GAG CAG AAG-3′), SRB1 (5′-TGG GGC TGC TGT TTG CTG CGC-3′ and 5′-CCA TGG TGA CCA GCG CCA AGG-3′), SREBF2 (5′-TAA CCC CTT GAC TTC CTT GCT-3′ and 5′-TGC TCT TAG CCT CAT CCT CAA-3′), HMG-CoA reductase (5′-AAT GCC TTG TGA TTG GAG TTG -3′ and 5′-CAG ACC CAA GGA AAC CTT AGC-3′), ABCG1 (5′-CCT GAA GAA GGT GGA CAA CAA-3′ and 5′-CTC CTG AAC AGT GAG GTG AGG-3′), apoA-I (5′-ACG TAT GGC AGC AAG ATG AAC-3′ and 5′-AGA GCT CCA CAT CCT CTT TCC-3′), apoE (5′-ACA AGA ACT GAC GGC ACT GAT-3′ and 5′-CGT ATC TCC TCT GTG CTC TGG-3′), apoA-V (5′-TGT CCCACA AAC TCA CAC GTA-3′ and 5′-TTT CCT CTG TCT CCT GGT CAA-3′), and β-actin (5′-CTG ACC CTG AAG TAC CCC ATT-3′ and 5′-TCT GCG CAA GTT AGG TTT TGT-3′) (synthesized by Hokkaido System Science, Japan). Quantification of mRNA for these primers products was accomplished by using SYBR Green PCR master mix reagent in an ABI PRISM 7700 sequence detection system (Applied Biosystems, Japan).

2.8. Other methods

Paragon Electrophoresis System (Beckman Coulter) was used for performing lipoprotein electrophoresis of mouse plasma. Mouse plasma LCAT activity was determined by measuring the decrease in plasma-free

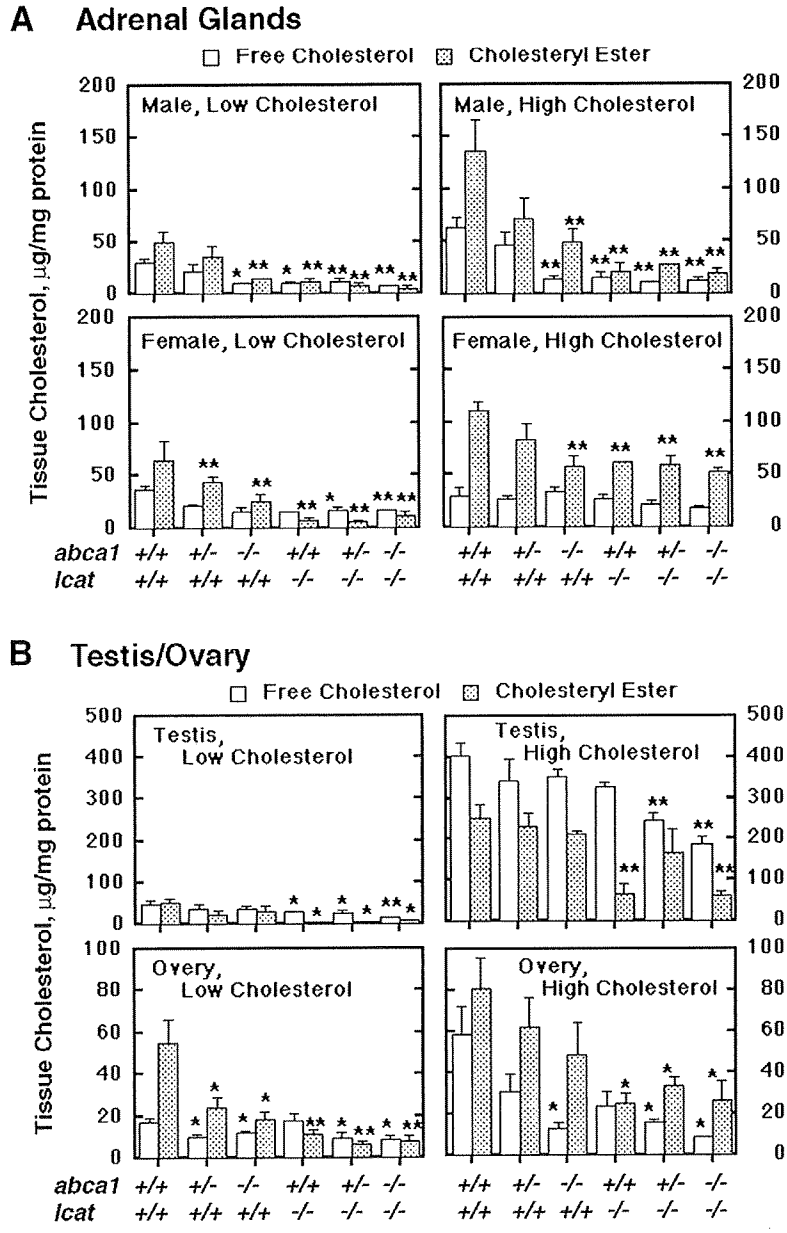

Fig. 2. Cholesterol content in the steroidogenic organs. (A) Cholesterol in adrenal glands. Cholesterol content of adrenal glands was determined for male and female mice with the six different genotypes (*abca1(+/+)lcat(+/+)*, *abca1(+/−)lcat(+/+)*, *abca1(−/−)lcat(+/+)*, *abca1(+/+)lcat(−/−)*, *abca1(+/−)lcat(−/−)*, and *abca1(−/−)lcat(−/−)*), after feeding normal low-cholesterol chow (0.2%) and high-cholesterol chow (1.2%) as described in the text ($n=4$ for each group). Adrenal glands were collected from the mouse after double perfusion as described in the text (first with PBS and then with 4% formaldehyde). Free cholesterol and CE were determined for the homogenized adrenal glands according to the methods described. (B) Cholesterol in testis and ovary. Cholesterol content of testis and ovary was determined for the six different genotypes as above of male and female fed with low- and high-cholesterol chow. The organs were collected, and cholesterol was measured as above. The data represent micrograms per milligram protein of cholesterol moiety. The values represent mean ± SD for four determinations (*$p<0.05$, **$p<0.01$ from the wild type).

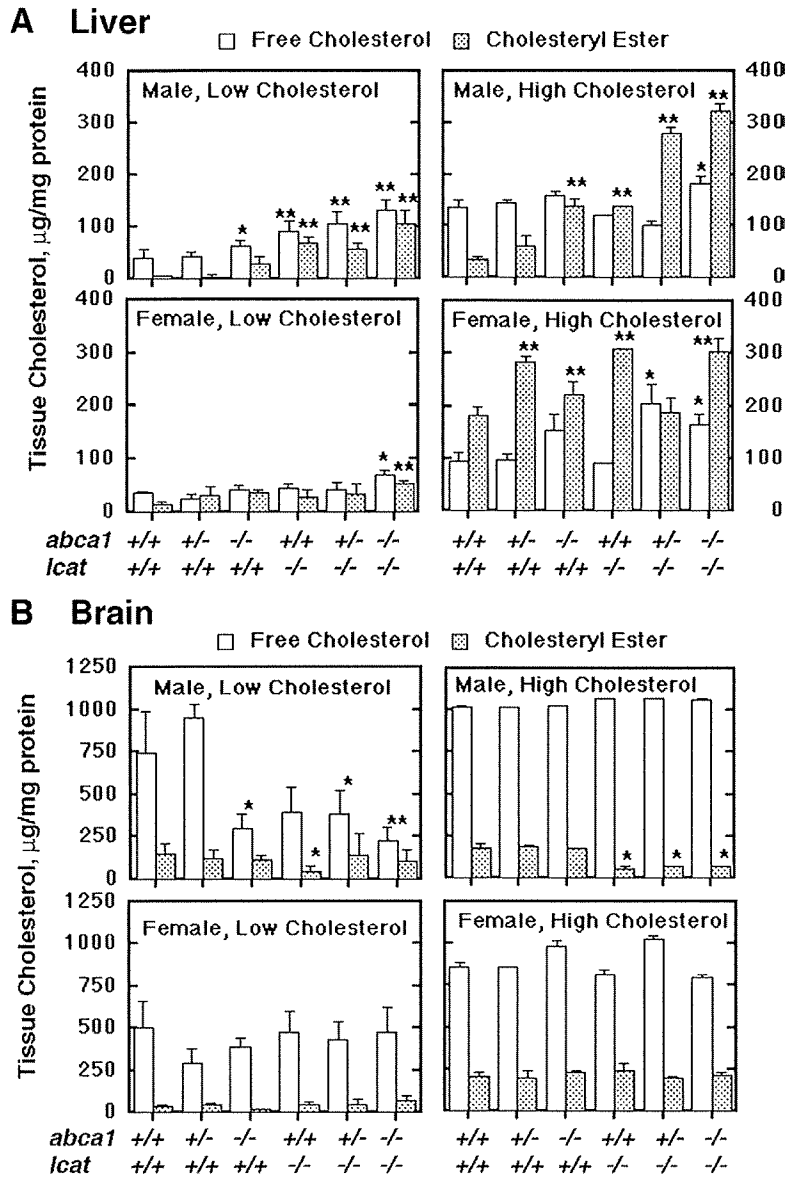

Fig. 3. Cholesterol content in the non-steroidogenic organs. Cholesterol content of the liver (A) and brain (B). The liver and brain were removed from the mice with six different genotypes (*abca1(+/+)lcat(+/+)*, *abca1(+/−)lcat(+/+)*, *abca1(−/−)lcat(+/+)*, *abca1(+/+)lcat(−/−)*, *abca1(+/−)lcat(−/−)*, and *abca1(−/−)lcat(−/−)*), male and female fed with normal chow and high-cholesterol chow, after whole body perfusion. Free cholesterol and cholesteryl ester were measured for the homogenized organs as described in the Methods section. The data represent micrograms per milligram protein of cholesterol moiety. The values represent mean ± SD for four determinations (*$p<0.05$, **$p<0.01$ from wild type).

cholesterol after incubating plasma in the presence of an additional artificial substrate of cholesterol/dimyristoylphosphatidylcholine vesicles using an assay kit "Anasolv LCAT" provided by Daiichi Pure Chemicals Co. Ltd. (Tokyo, Japan) according to the manufacturer's instruction [23]. Protein content was determined with a bicinchoninic acid assay reagent (Pierce) using BSA as a standard. Statistical analysis was performed by using 2-tailed Student's *t* test for unpaired comparisons to evaluate significance of the differences between the groups.

3. Results

3.1. Basic characterization of ABCA/LCAT-deficient mice

Genotypes for *abca1* and *lcat* of mouse were determined as described in the Methods section and the phenotypes based on these genotypes were confirmed by measuring plasma lipoprotein profiles and LCAT activities (examples are shown in Supplementary Figure I). Mice with the six genotypes were used for further experimental analysis: *abca1(+/+)lcat(+/+)* (wild type), *abca1(+/−)lcat(+/+)*, *abca1(−/−)lcat(+/+)*, *abca1(+/+)lcat(−/−)*, *abca1(+/−)lcat(−/−)*, and *abca1(−/−)lcat(−/−)*. Supplementary Table I lists the body weight of the animals. The mutations cause decreasing tendency of the body weight and this was most apparent in the *abca1(−/−)lcat(−/−)* genotype.

Supplementary Figure II shows the results of HPLC analysis of plasma lipoprotein of the mice with each genotype. Being consistent with previous findings, it shows a moderate and marked decrease in HDL in *abca1(+/−)* and *abca1(−/−)* mice in the *lcat(+/+)* background, respectively. HDL markedly decreased also in *lcat(−/−)* mice. Choline-phospholipid associated with serum protein markedly decreased in the *lcat(−/−)* genotypes presumably reflecting the decrease in lysophosphatidylcholine in lack of the LCAT

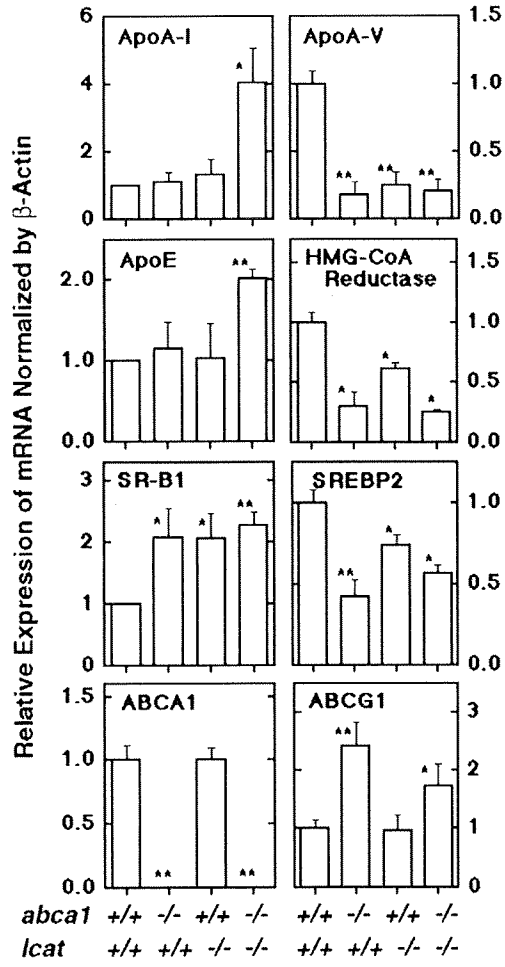

Fig. 4. Real-time quantitative PCR for the liver mRNA. Messenger RNA was collected from the liver of the mice with four genotypes (*abca1(+/+)lcat(+/+)*, *abca1(−/−)lcat(+/+)*, *abca1(+/+)lcat(−/−)*, and *abca1(−/−)lcat(−/−)*) ($n=3$ for each group) and converted to cDNA through reverse transcription according to the method described in the text. Expressions of the mRNA for apoA-I, apoA-V, apoE, HMG-CoA reductase. SR-B1, SREBP2, ABCA1, and ABCG1, were determined by real-time quantitative PCR. The results were normalized for the mRNA levels of β-actin. The values represent mean ± SD for three determinations (*p<0.05, **p<0.01 from wild type).

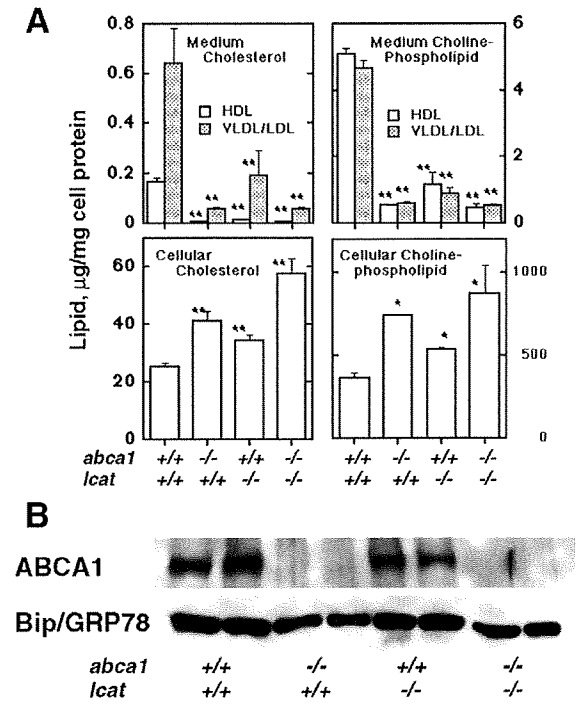

Fig. 5. HDL biogenesis from the mouse hepatocytes in primary culture. Primary hepatocytes were isolated from the mice with four different genotypes (*abca1(+/+)lcat(+/+)*, *abca1(−/−)lcat(+/+)*, *abca1(+/+)lcat(−/−)*, and *abca1(−/−)lcat(−/−)*) ($n=2$ for each group) and cultured in 10% FBS containing Dulbecco's modified Eagle medium (DMEM) described in the Methods section. The cells were exposed to DMEM containing 0.02% BSA for 16 hours. (A) The conditioned medium was fractionated by ultracentrifugation as described in the text and cholesterol and choline phospholipid were measured for HDL ($d=1.063$–1.21) and VLDL/LDL ($d<1.063$) fractions. The values represent mean ± SD for four determinations (*p<0.05, **p<0.01 from wild type). (B) Western blotting analysis of ABCA1 of the cell membrane and Bip/GRP78 as a loading internal control.

reaction in plasma. The mice were fed with normal chow (low cholesterol, 0.2%) and with high-cholesterol chow (1.2%), and plasma lipoproteins were analyzed by ultracentrifugation (Table 1). HDL was markedly decreased in the *abca1(−/−)* and *lcat(−/−)* mice and moderately in the *abca1(+/−)lcat(+/+)* mice. LDL/VLDL fraction was not much influenced by the mutations except for the decrease in its cholesterol in the *abca1(−/−)lcat(−/−)* mice.

3.2. HDL metabolism

HDL metabolism in plasma was investigated by measuring clearance of its CE tracing radiolabeled cholesteryl ether in HDL injected into the animals fed with normal chow. As shown in Fig. 1A, clearance rate of HDL cholesteryl ether was two-fold faster in the *abca1(−/−)* and *lcat (−/−)* mice and four-fold faster in the *abca1(−/−)lcat(−/−)* mice. Deposition of the radiolabeled cholesteryl ether originating in the HDL was in the order of its clearance rate, but deposition of the HDL–CE was in the order of the plasma HDL level when evaluated by using a specific ratio activity of CE at 30 minutes after the injection (Fig. 1B) assuming that the metabolic fate of cholesteryl ether in HDL is the same as that of CE before its hydrolysis.

3.3. Cholesterol accumulation in the body

Cholesterol contents in the various organs were measured in the animals fed with normal chow and high-cholesterol chow. Fig. 2 shows the results in steroidogenic organs of adrenal glands and testis/ovary. In each condition, cholesterol contents decreased as the plasma HDL level decreased by genetic mutations. In contrast, cholesterol increased in the liver when either the *abca1* or the *lcat* gene was disrupted, and this was more apparent when both genes were impaired (Fig. 3A). Cholesterol tended to decrease in most of the organs such as kidneys, thymus, lung, spleen and heart muscle of the animals with disruption of either genes under normal chow feeding, and this was recovered by high-cholesterol chow feeding (Supplementary Table II). Interestingly, decrease in cholesterol was also seen in the male brain but not in the female by the gene disruptions except for the *abca1(+/−)lcat(+/+)* mice, and this change was reversed when feeding with high-cholesterol chow (Fig. 3B).

3.4. Other cholesterol-related genes

Expressions of other cholesterol-related genes were estimated in the mouse liver when the *abca1* and *lcat* genes were mutated (Fig. 4). The mRNA levels for apoA-I and apoE were increased only in the *abca1(−/−)lcat(−/−)* genotype. On the other hand, scavenger receptor B1 (SR-B1) mRNA increased also in *abca1(−/−)lcat(+/+)*

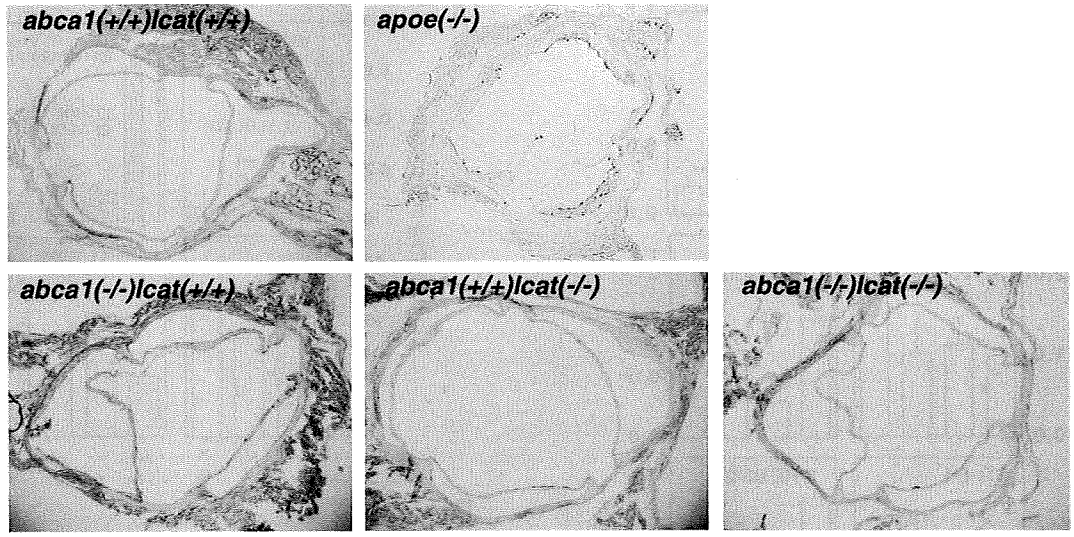

Fig. 6. Vascular lipid deposition. The heart was collected from the high-cholesterol chow-fed mice with four different genotypes of *abca1* and *lcat* (*abca1(+/+)lcat(+/+)*, *abca1(−/−)lcat(+/+)*, *abca1(+/+)lcat(−/−)*, and *abca1(−/−)lcat(−/−)*) as well as the mice with apoE deficiency. The organ was frozen, and the aortic valve region specimen was obtained and stained with Oil red O as described in the text.

and *abca1(+/+)lcat(−/−)*.ABCG1 mRNA increased only when the *abca1* gene was disrupted and not when the *lcat* gene was mutated. The mRNAs of HMG-CoA reductase and sterol regulatory element binding protein (SREBP) 2 were decreased being consistent with their regulation through the SREBP systems. Expression of the apoA-V gene decreased in mice with either mutant gene, being inconsistent with previous findings that this gene is regulated by PPARs and LXRs [24–26]. Interestingly, ABCA1 mRNA did not change in the *lcat (−/−)* genotype in spite of the decrease in hepatic cell cholesterol. This may be a reflection of the dual regulation of the *abca1* gene in hepatocytes by the LXR and SREBP systems [27].

3.5. Hepatic production of HDL

Production of lipoprotein was examined by using primary hapatocytes isolated from the animals (Fig. 5). Production of HDL was markedly decreased not only in the genotypes of *abca1(−/−)lcat(+/+)* and *abca1(−/−)lcat(−/−)* but also in the *abca1(+/+)lcat(−/−)* genotype. Expression of ABCA1 protein was not significantly decreased in the *abca1(+/+)lcat(−/−)* in agreement with the results of its mRNA expression. There must be an additional factor(s) to down-regulate hepatic HDL production in congenital disruption of the *lcat* gene.

3.6. Vascular lesions

Finally, vascular lipid accumulation was estimated in the high-cholesterol chow-fed groups. There was no apparent increase in lipid accumulation in the aortic intima in any genotype animals. It was further investigated by histological lipid staining with Oil Red O in the aortic valve region where lipid accumulates most sensitively. Fig. 6 demonstrates that there was no significant lipid accumulation in the mice of any genotype, comparing with a positive control of the finding in an apoE-deficient mouse.

4. Discussion

We characterized the phenotypes of mice having deficiency of ABCA1 and LCAT, the two key factors to regulate cell cholesterol released to maintain cholesterol homeostasis. The results are summarized as follows: 1) Plasma HDL was markedly decreased in each single deficiency and yet additive in the double deficiency. 2) Clearance of exogenously injected HDL-CE increased in each single deficiency and additively increased in the double deficiency, while overall CE deposit from HDL to the organs was dependent on the plasma HDL level. 3) Cholesterol content in the organs including the brain was dependent on plasma HDL levels in the normal chow-fed condition but this was cancelled by high-cholesterol feeding, including in the brain. 4) Cholesterol content was increased in each single deficiency in the liver, and further increased in the double deficiency. Changes in expression of the cholesterol-related gene in the liver reflected the increase in cellular cholesterol. 5) Hepatic HDL production decreased not only in the ABCA1 deficiency but also in the LCAT deficiency in spite of the increase in apoA-I expression and no change in ABCA1 expression for unknown reason. 6) Vascular cholesterol deposit in short term was not increased even in the double deficiency.

The results were largely consistent with our previous findings when ABCA1 was inhibited by probucol in the LCAT-deficient mice; severe reduction of plasma HDL without systemic cholesterol deposit, but rather with reduction in cholesterol storage especially in the steroidogenic organs and increase in hepatic cholesterol [16]. In this previous work, we concluded that the main cholesterol carrier among the organs is HDL in mouse, including the delivery of cholesterol to the steroidogenic organs. On the other hand, hepatic cholesterol accumulation by inhibiting ABCA1 in the LCAT-deficient mouse indicated that the main HDL production site is the liver in mouse. We also speculated that cholesterol transport from extrahepatic organs to the liver for its catabolism can be carried out even without HDL. However, one might concern about the potential unknown effects of probucol in this experimental design since this drug is known for various unexpected clinical effects potentially related to its strong anti-oxidative nature. In the present paper, we therefore introduced a genetic defect of ABCA1 instead of its pharmacological inhibition and yielded similar results. Our speculation in the previous paper about cholesterol transport in vivo [16] has been confirmed. The apparent increase in clearance of exogenous HDL-CE indicates the increase in cellular cholesterol demand when plasma HDL is severely reduced in mice, and this seems highly sensitive in differentiating between the single-gene deficiencies and the double-gene defect.

In addition to these parameters, we evaluated the expression of several cholesterol-related genes in the liver. While the results were mostly consistent with the increase in cholesterol in the liver by the